Role of Color in Histological Image Analysis

Rough-Fuzzy Computing to Deep Learning

Pradipta Maji

Machine Intelligence Unit
Indian Statistical Institute, Kolkata, INDIA
E-mail:pmaji@isical.ac.in
Web:www.isical.ac.in/~pmaji

International Joint Conference on Rough Sets – 2023 @Krakow, Poland

Outline of the Talk

- Histological Image Analysis
- Importance of Color
- Normalization of Color
- Rough-Fuzzy Clustering
- Deep Learning
- Conclusions

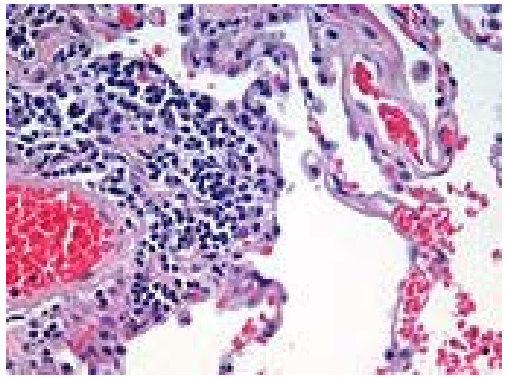

Histology Image Analysis

- In histology, microscopic images of tissue sections are examined to study the manifestation of diseases under consideration.

- Most important property of histological images, as compared to radiological, cytological and other imaging modalities, is
  - enormous density of data,
  - more cellular details.

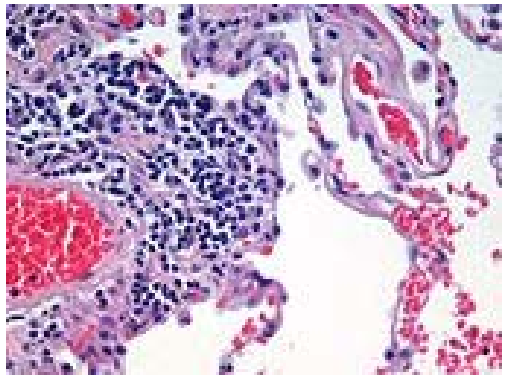

Cell nuclei (blue-purple), red blood cells (bright red), other cell bodies and extracellular material (pink), and air spaces (white).

- It makes computer-aided diagnosis more accurate than other imaging modalities.

Histology Image Analysis

- When a pathologist looks at a biopsy of a suspected cancer, the histological section (tissue sample) is stained with multiple contrasting histochemical reagents, which highlight different tissue structures and cellular features.

- Haematoxylin and eosin (H&E) stain is
  - one of the principal tissue stains used in histology.
  - gold standard in medical diagnosis.

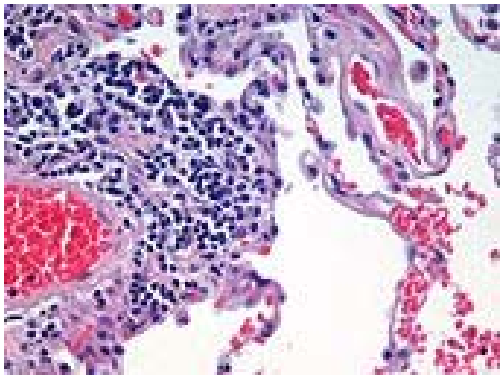

Cell nuclei (blue-purple), red blood cells (bright red), other cell bodies and extracellular material (pink), and air spaces (white).

- Haematoxylin stains cell nuclei a purplish blue, and eosin stains the extracellular matrix and cytoplasm pink, with other structures taking on different shades, hues, and combinations of these colors.

Histology Image Analysis

- Hence, color in pathology plays a pivotal role as a good indicator of histological components.
  - Pathologist / pattern recognition system can easily differentiate between nuclear and cytoplasmic parts of a cell.

- Problem of histological tissue analysis: Inadmissible inter and intra-specimen variation in stained tissue color.

UCSB Breast Cancer Cell Data: H&E stained

Biopsy 1

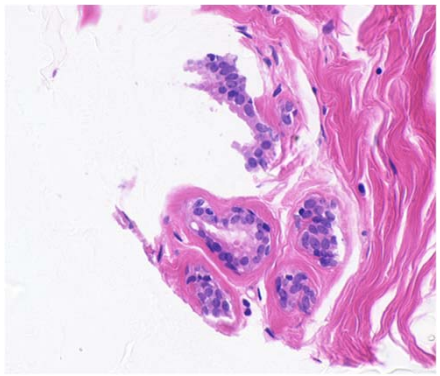

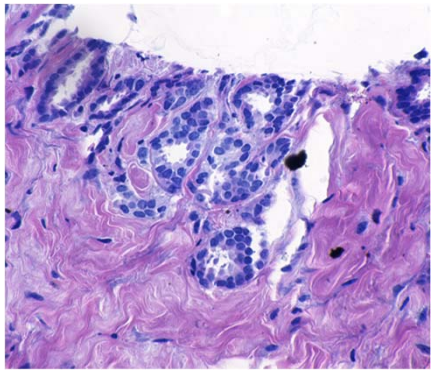

Biopsy 8

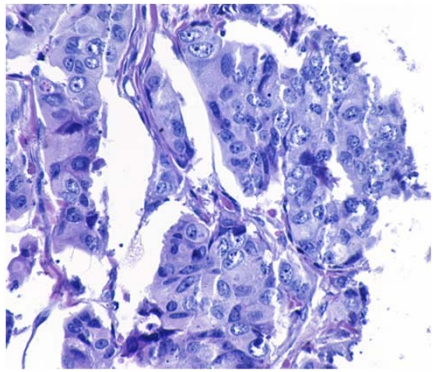

Factors Responsible for Color Inconsistency

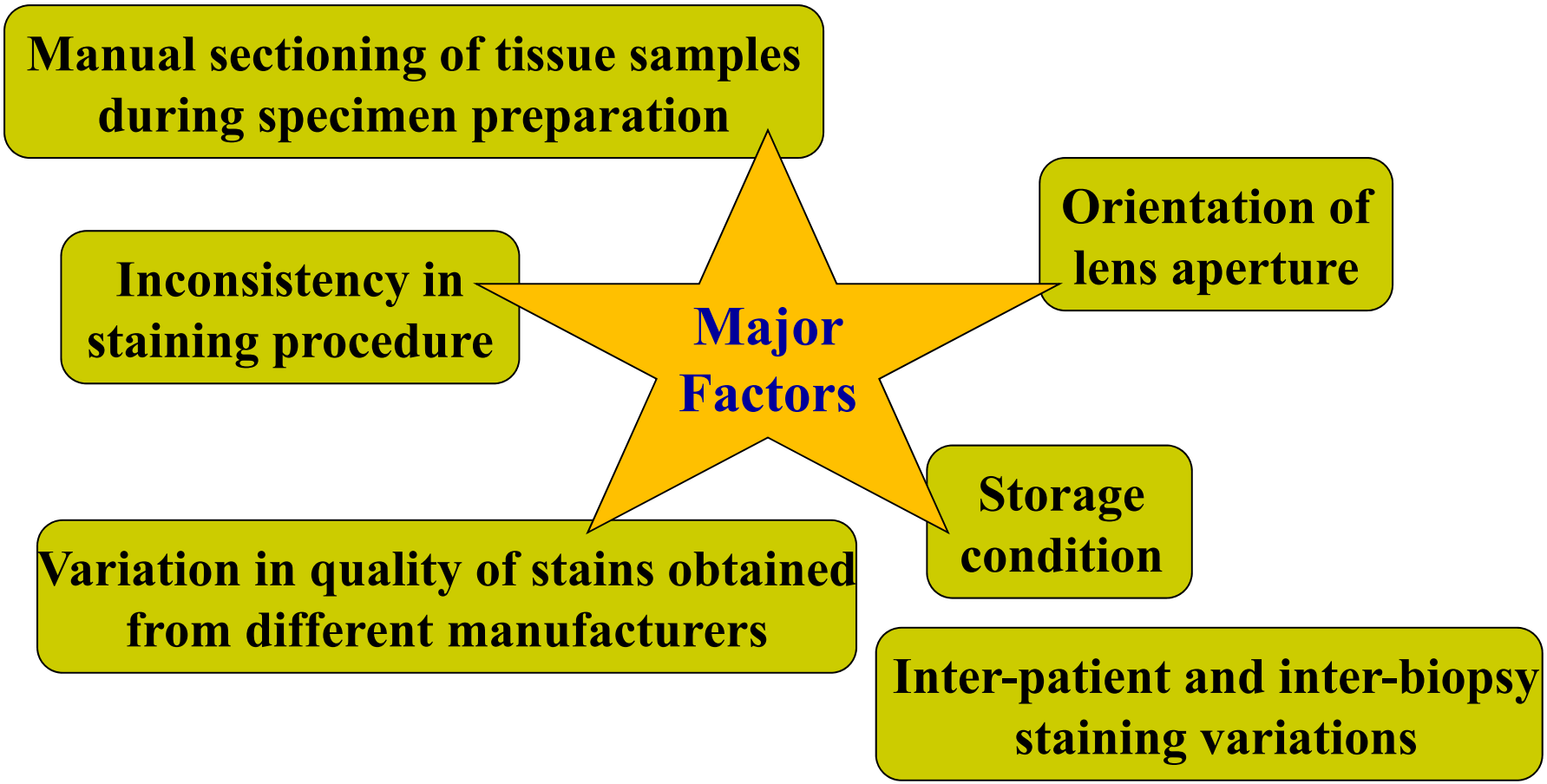

Impact of Dust

- Presence of artefacts in the histology images due to dust particles

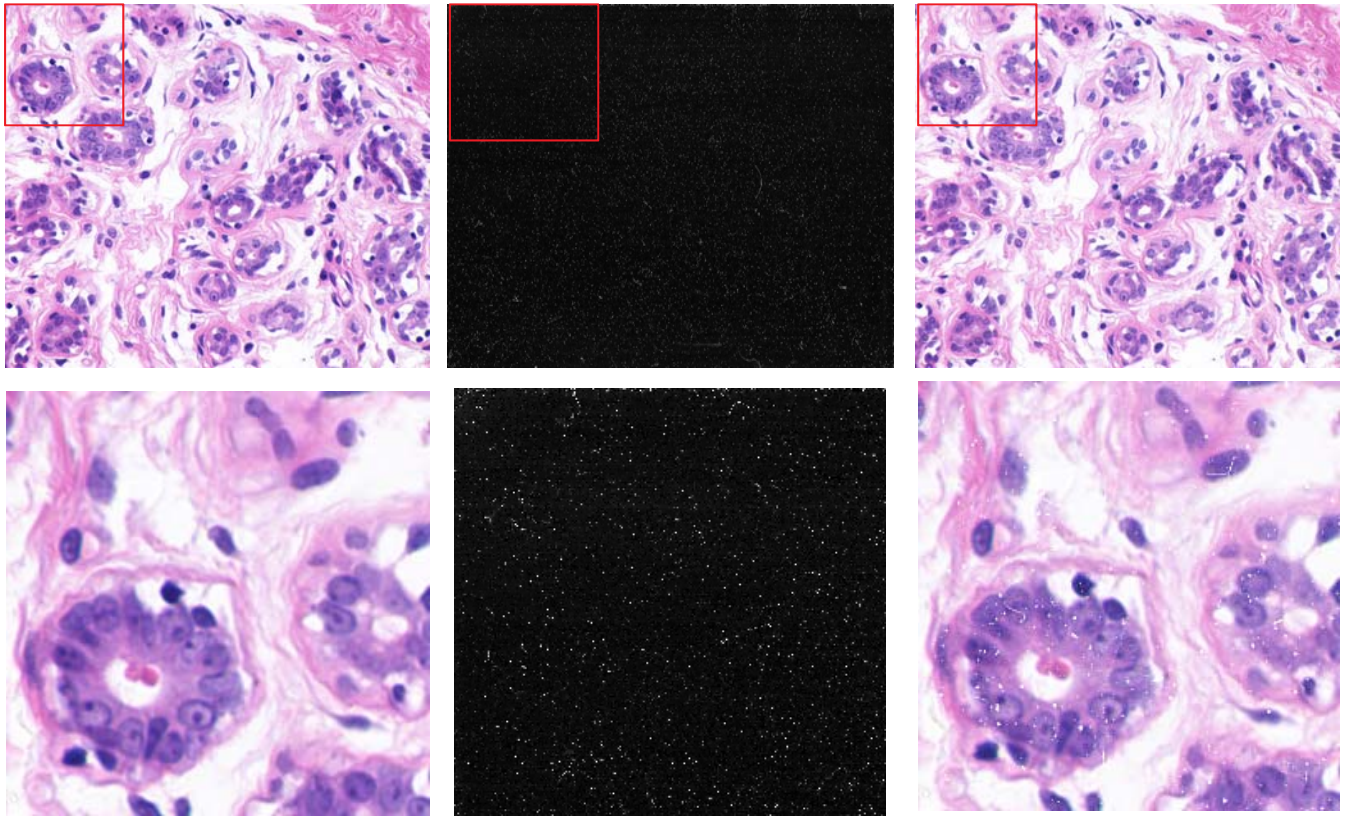

Original **Dust film** **Dust added**

Effect of Fading

- Color variation due to fade color effect: It happens when the histology slides are unused for many days.

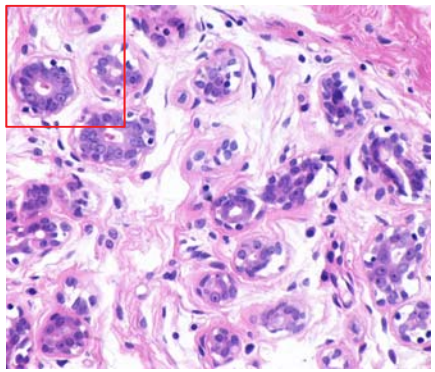

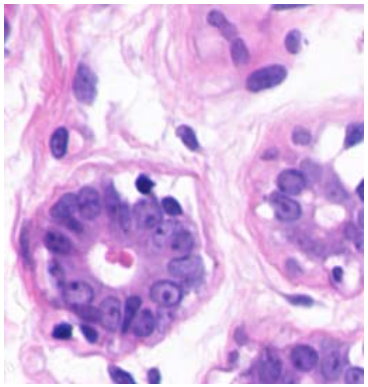

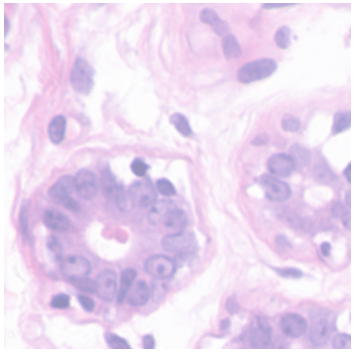

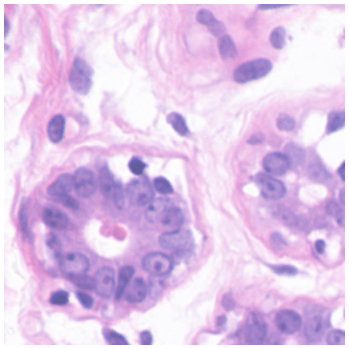

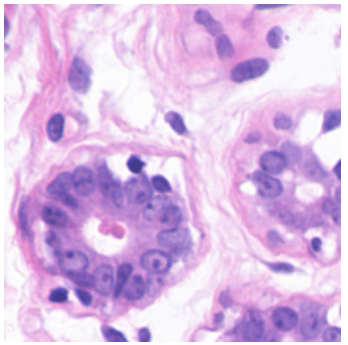

Opacity=10 **Opacity=25** **Opacity=50** **Opacity=75** **Opacity=90**

Why Color Normalization?

- Color inconsistency present among histological images, collected from different sources, may significantly affect the performance of computer-aided diagnosis.

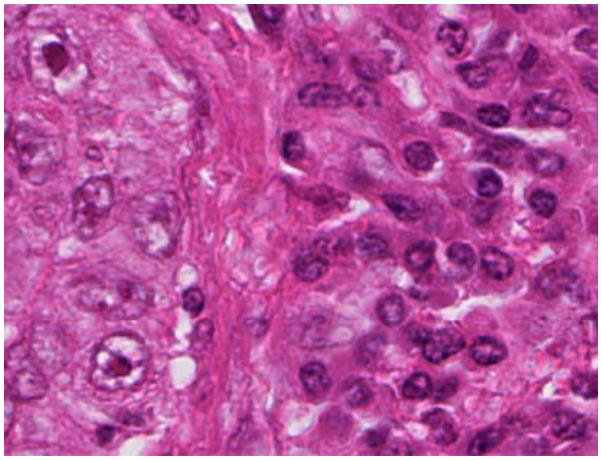

Hamamatsu Nanozoomer

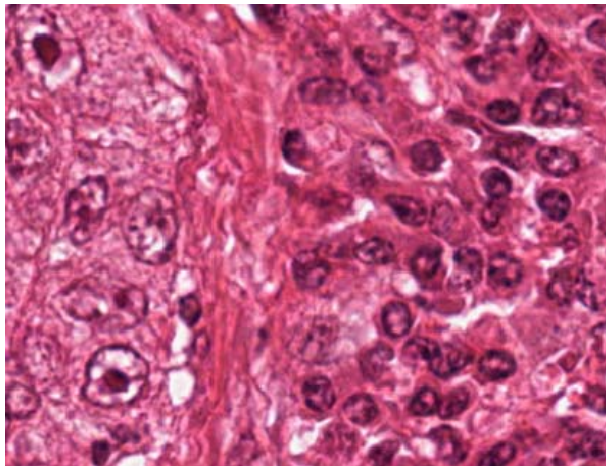

Aperio Scanscope

Image courtesy: http://camper.in.tum.de/Students/MaBaDaHistologyProcess

Why Color Normalization?

- Color inconsistency present among histological images, collected from different sources, may significantly affect the performance of computer-aided diagnosis.

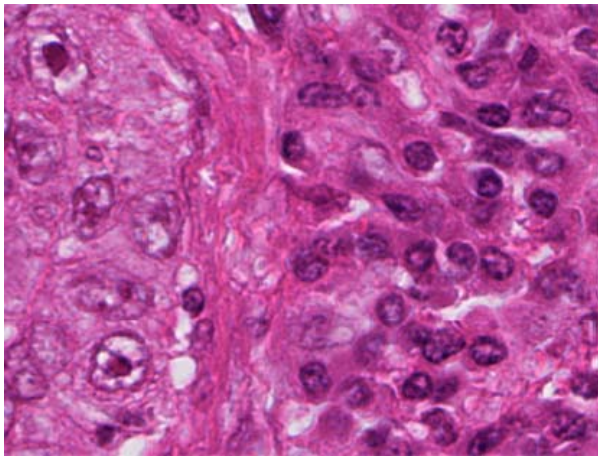

Hamamatsu Nanozoomer

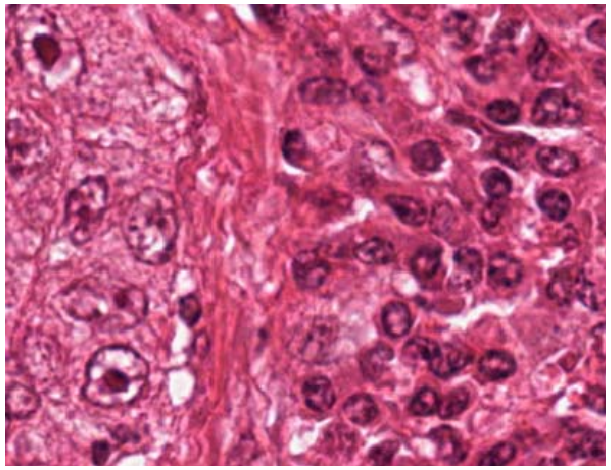

Aperio Scanscope

Challenge: How to reduce color variation present among the images within a particular biopsy set.

Image courtesy: http://camper.in.tum.de/Students/MaBaDaHistologyProcess

Why Color Normalization?

- Histological information consists of morphological information and details of in-situ molecular and cellular structures, which is very important in therapeutic diagnosis.

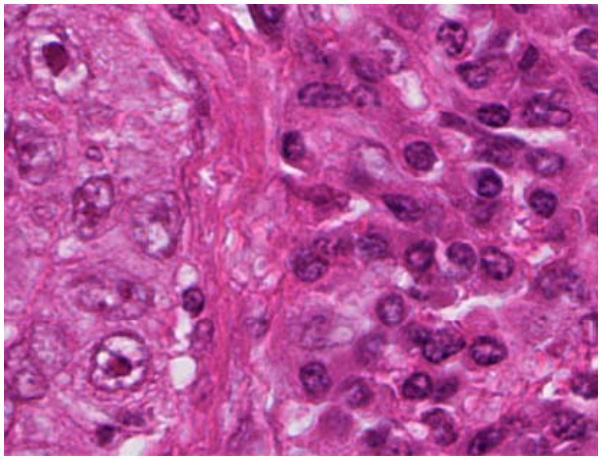

Hamamatsu Nanozoomer

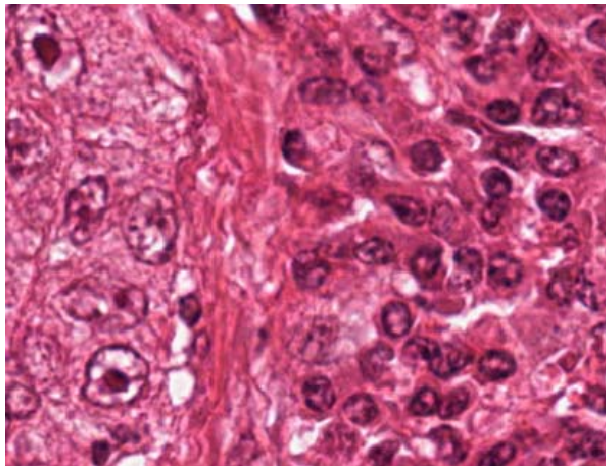

Aperio Scanscope

Image courtesy: http://camper.in.tum.de/Students/MaBaDaHistologyProcess

Why Color Normalization?

- Histological information consists of morphological information and details of in-situ molecular and cellular structures, which is very important in therapeutic diagnosis.

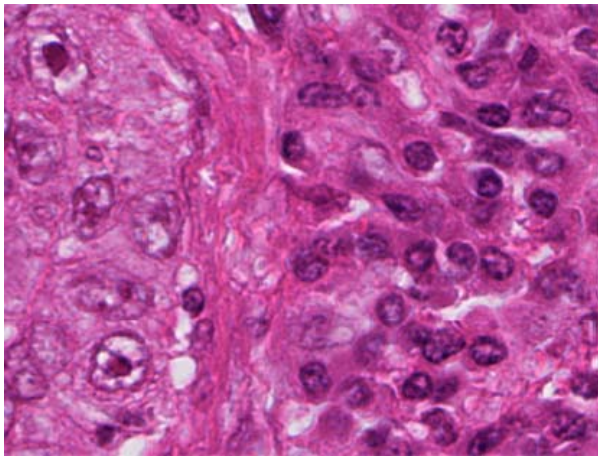

Hamamatsu Nanozoomer

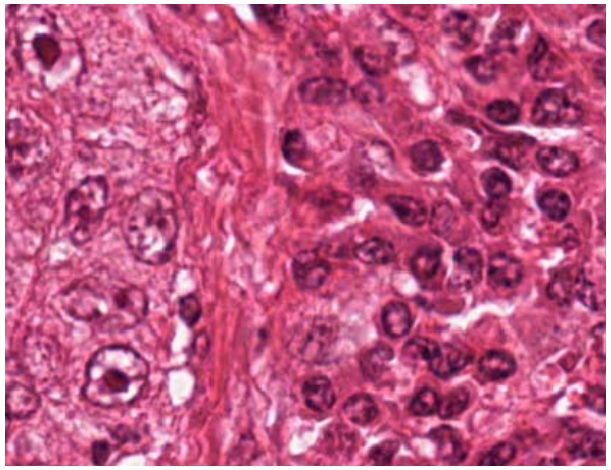

Aperio Scanscope

Challenge: Reduce color disagreement without hampering histological information in the images.

Image courtesy: http://camper.in.tum.de/Students/MaBaDaHistologyProcess

Definition of the Problem

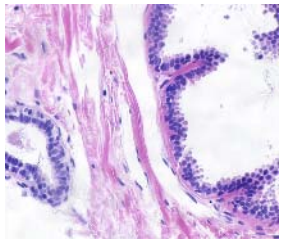

Source

Color Normalization

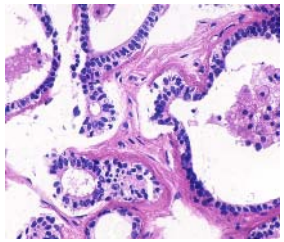

Template

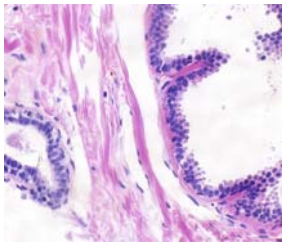

Normalized

Color / Stain Transfer ← Color Normalization → Stain Estimation / Separation

Supervised ← Color Normalization → Unsupervised

Clustering for Color Normalization

- Clustering is performed on HSI color space.

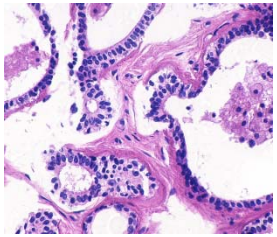

Histology image

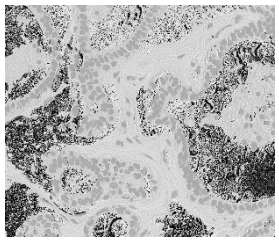

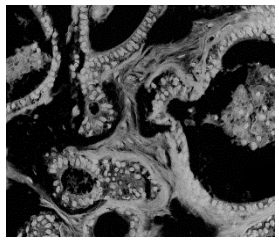

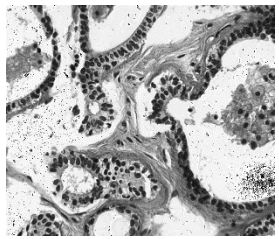

Hue: representative of color

range: $0 \leq \theta < 2\pi$, circular in nature

Saturation: contains stain bound information

Intensity: intensity/ value information

Clustering for Color Normalization

- Clustering is performed on weighted hue histogram.

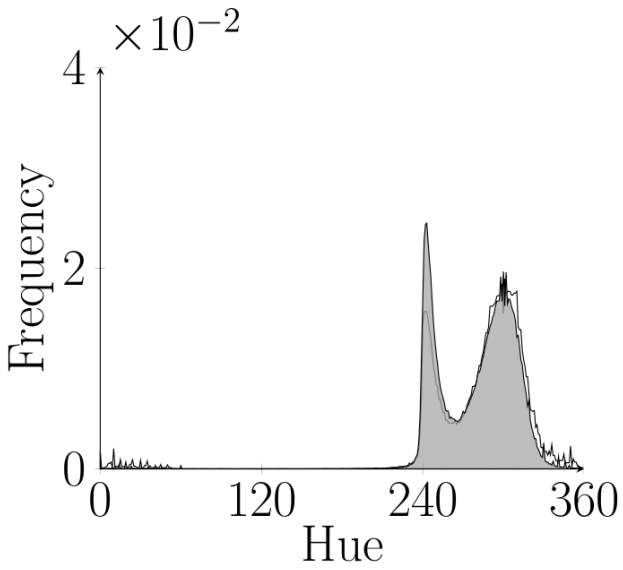

Hue histogram

why not standard hue histogram?

a number of sharp ridges attributed by achromatic pixels

ill-defined: small or insignificant saturation values

Solution??

Clustering for Color Normalization

- Clustering is performed on weighted hue histogram.

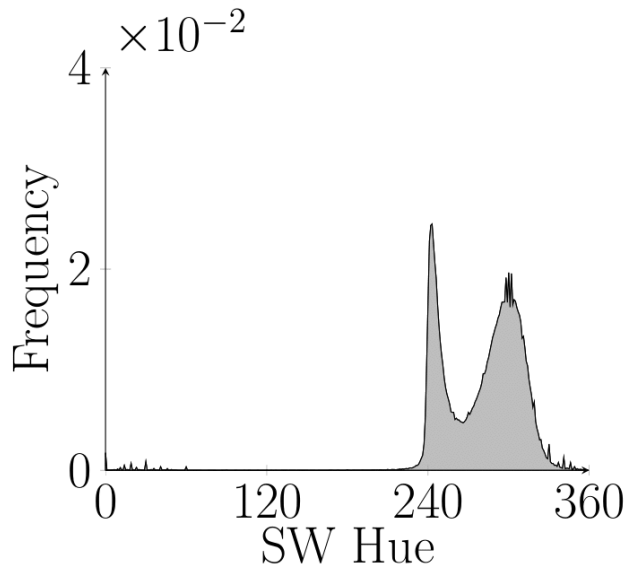

SW Hue histogram

$$H^{SW}(\theta) = \sum_{k \in I} s_k \delta(\theta, h_k)$$

$$\text{where, } \delta(\theta, h_k) = \begin{cases} 1 & \text{if } \theta = h_k \\ 0 & \text{otherwise} \end{cases}$$

reduces effects of achromatic pixels

Only SW hue histogram?

no local neighbourhood information

A. Hanbury, "Circular statistics applied to colour images", ***Computer Vision Winter Workshop***, 91(1-2), pp. 53-71, 2003.

Clustering for Color Normalization

- Clustering is performed on weighted hue histogram.

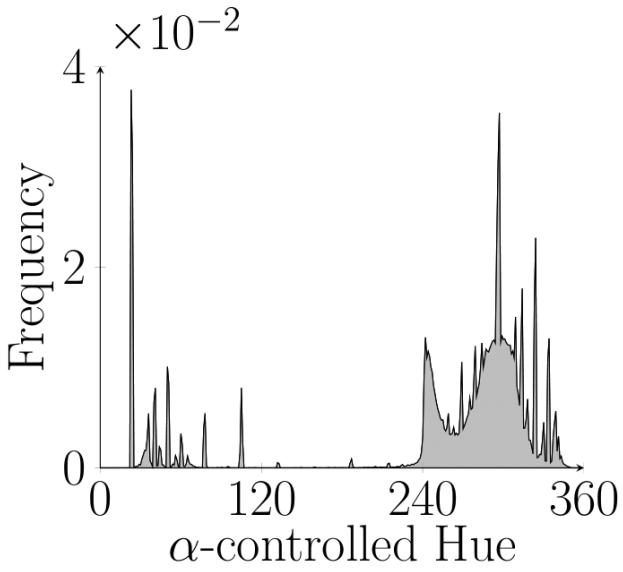

α-controlled Hue histogram

like linear space, local neighborhood information is computed as follows:

$$\xi_k = \frac{1}{1+\alpha}\left(h_k + \frac{\alpha}{|N_k|}\sum_{h_j \in N_k} h_j\right)$$

Solution??

Clustering for Color Normalization

- Clustering is performed on weighted hue histogram.

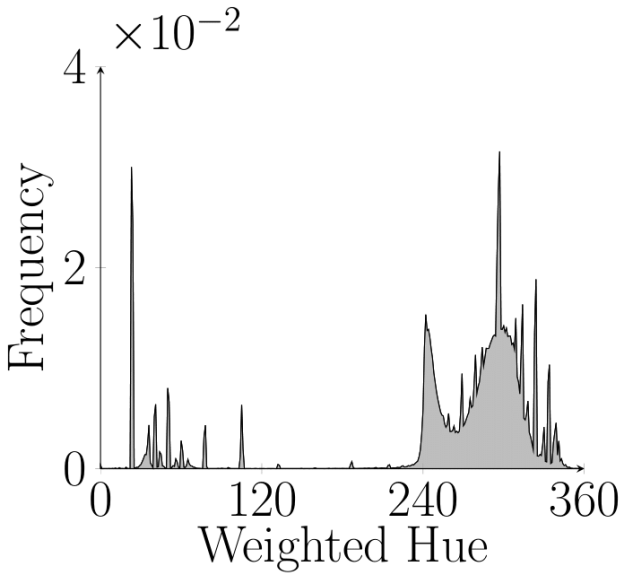

Weighted Hue histogram

Combing both, Weighted Hue histogram *H* is defined as:

$$H(\theta) = \frac{1}{2}\left[H^{SW}(\theta) + H^{\alpha}(\theta)\right]$$

incorporates both saturation weighted hue information and local neighbourhood information

P. Maji and S. Mahapatra, "Circular Clustering in Fuzzy Approximation Spaces for Color Normalization of Histological Images", ***IEEE Transactions on Medical Imaging***, vol. 39, no. 5, pp. 1735-1745, 2020.

Cosine Distance

- Clustering can be performed based on cosine distance.

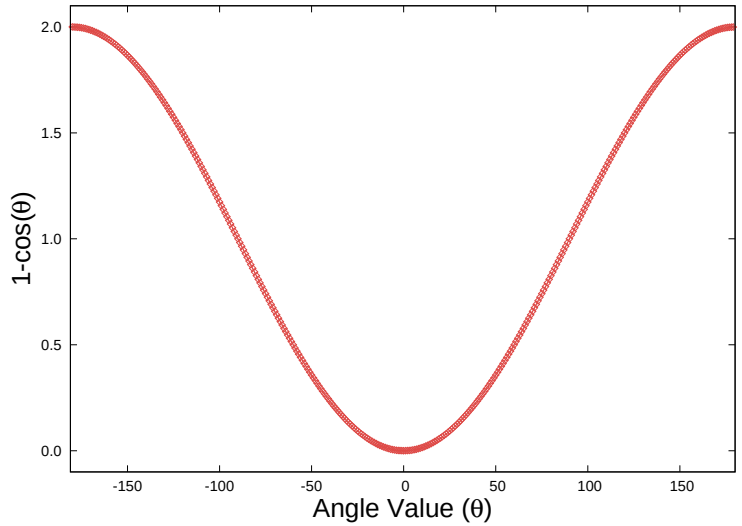

Cosine distance

why not cosine distance?

fails to model concentration of hue values near its peak

cannot capture inherent data distribution

Solution??

New Dissimilarity Measure

- Clustering is performed based on a new dissimilarity measure.

$$d(\theta_i,\theta_j)=\log\left(2\pi I_0(\kappa)\right)-\kappa\cos\left(\theta_i-\theta_j\right)$$

$$I_0(\kappa)=\frac{1}{2\pi}\int_0^{2\pi}\exp\left(\kappa\cos\theta\right)d\theta$$

***I_0(.)* is the modified Bessel function of first kind and order zero.**

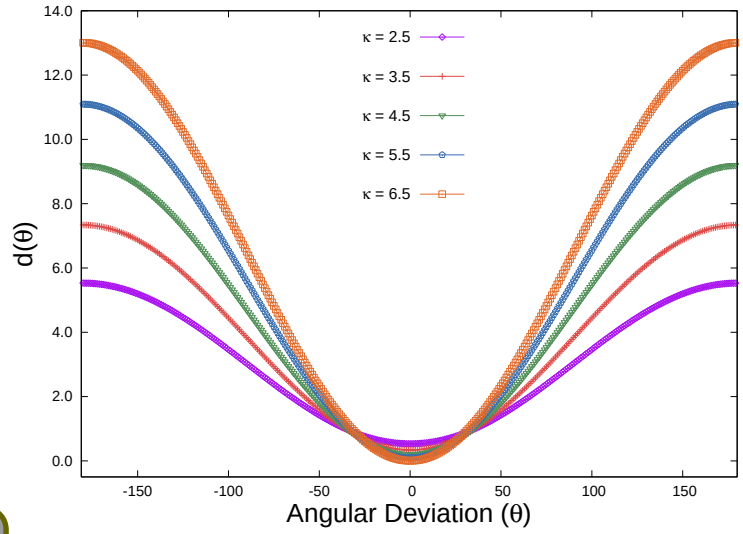

area under the curve is varied using κ without affecting periodicity

can capture intrinsic data distribution

1) $d(\theta_i,\theta_j)=d(\theta_j,\theta_i)$

2) $d(\theta_i,\theta_i)<d(\theta_i,\theta_j)\forall j\neq i$

3) $d(\theta_i,\theta_k)\leq d(\theta_i,\theta_j)+d(\theta_j,\theta_k)\forall\,\theta_i,\theta_j,\theta_k\in[0,2\pi)$

connection with von Mises probability distribution

Rough-Fuzzy Circular Clustering

- A rough-fuzzy clustering in circular domain

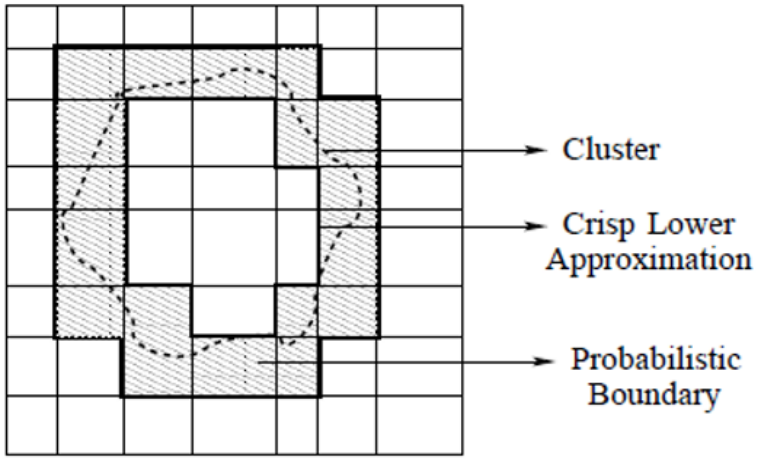

Why fuzzy clustering?

due to staining routine and storage condition, stains become overlapped

Fuzzy set: to deal with overlapping nature of stains

Why rough set?

Rough set: deals with uncertainly and incompleteness in class definition

L. A. Zadeh, "Fuzzy Sets: Information and Control", vol. 24, no. 3, pp. 338-353, 1965.
Z. Pawlak, "Rough Sets: Theoretical Aspects of Reasoning About Data", Dordrecht, The Netherlands: Kluwer, 1991.

Objective Function

Minimization of objective function with respect to parameter set ψ:

$$J_{RF}(\psi)=\sum_{i=1}^{c}\left[\omega\times J_i^L(\psi)+(1-\omega)\times J_i^B(\psi)\right]$$

$$\psi=\left\{\nu_{ij},\mu_i,\kappa_i\right\}$$

corresponding to lower approximation region for *i*-th class:

$$J_i^L(\psi)=\sum_{\theta_j\in\underline{A}(\beta_i)}\left[\log\left(2\pi I_0(\kappa_i)\right)-\kappa_i\cos\left(\theta_j-\mu_i\right)\right]H(\theta_j)$$

corresponding to boundary region for *i*-th class:

$$J_i^B(\psi)=\sum_{\theta_j\in B(\beta_i)}\nu_{ij}^m\left[\log\left(2\pi I_0(\kappa_i)\right)-\kappa_i\cos\left(\theta_j-\mu_i\right)\right]H(\theta_j)+\sum_{\theta_j\in B(\beta_i)}\left[\nu_{ij}^m\log\left(\nu_{ij}^m\right)-\nu_{ij}^m\right]H(\theta_j)$$

Estimation of Membership Function

$$\frac{\partial J_{RF}(\psi)}{\partial \nu_{ij}} = 0 \quad \Rightarrow \quad \nu_{ij} = \left[\frac{\exp\{\kappa_i \cos(\theta_j - \mu_i)\}}{2\pi I_0(\kappa_i)} \right]^{\frac{1}{m}}$$

So, fuzzy membership function follows von Mises distribution

Von Mises probability distribution:

$$vM(\mu, \kappa) = \frac{1}{2\pi I_0(\kappa)} \exp\{\kappa \cos(\theta - \mu)\}$$

$$\mu \in [0, 2\pi) \qquad \kappa > 0$$

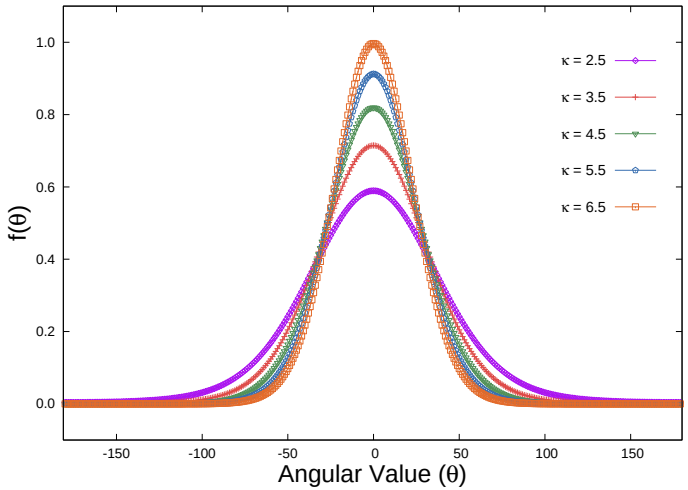

N. I. Fisher, "Statistical Analysis of Circular Data", *Cambridge University Press*, Cambridge, U.K., 1995.

Estimation of Stain Representative

$$\frac{\partial J_{RF}(\psi)}{\partial \mu_i} = 0$$

$$\mu_i = \arctan\left[\frac{\omega \times \sum_{\theta_j \in \underline{A}(\beta_i)} \sin(\theta_j) H(\theta_j) + (1-\omega) \times \sum_{\theta_j \in B(\beta_i)} \nu_{ij}^m \sin(\theta_j) H(\theta_j)}{\omega \times \sum_{\theta_j \in \underline{A}(\beta_i)} \cos(\theta_j) H(\theta_j) + (1-\omega) \times \sum_{\theta_j \in B(\beta_i)} \nu_{ij}^m \cos(\theta_j) H(\theta_j)}\right]$$

It depends on the choice of relative importance parameter ω

Estimation of Concentration Parameter

$$\frac{\partial J_{RF}(\psi)}{\partial \kappa_i} = 0$$

$$\kappa_i = \mathrm{T}^{-1}\left[\frac{\omega \times \sum_{\theta_j \in \underline{A}(\beta_i)} \cos(\theta_j - \mu_i) H(\theta_j) + (1-\omega) \times \sum_{\theta_j \in B(\beta_i)} \nu_{ij}^m \cos(\theta_j - \mu_i) H(\theta_j)}{\omega \times \sum_{\theta_j \in \underline{A}(\beta_i)} H(\theta_j) + (1-\omega) \times \sum_{\theta_j \in B(\beta_i)} \nu_{ij}^m H(\theta_j)}\right]$$

$$\mathrm{T}(\kappa_i) = \frac{I_1(\kappa_i)}{I_0(\kappa_i)}$$

T^{-1}(.) is approximated using numerical methods

N. I. Fisher, "Statistical Analysis of Circular Data", *Cambridge University Press*, Cambridge, U.K., 1995.

Color Normalization Method

Template

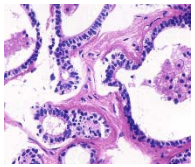

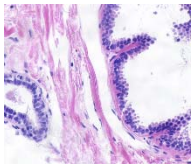

Source

P. Maji and S. Mahapatra, "Circular Clustering in Fuzzy Approximation Spaces for Color Normalization of Histological Images", ***IEEE Transactions on Medical Imaging***, vol. 39, no. 5, pp. 1735-1745, 2020.

Color Normalization Method

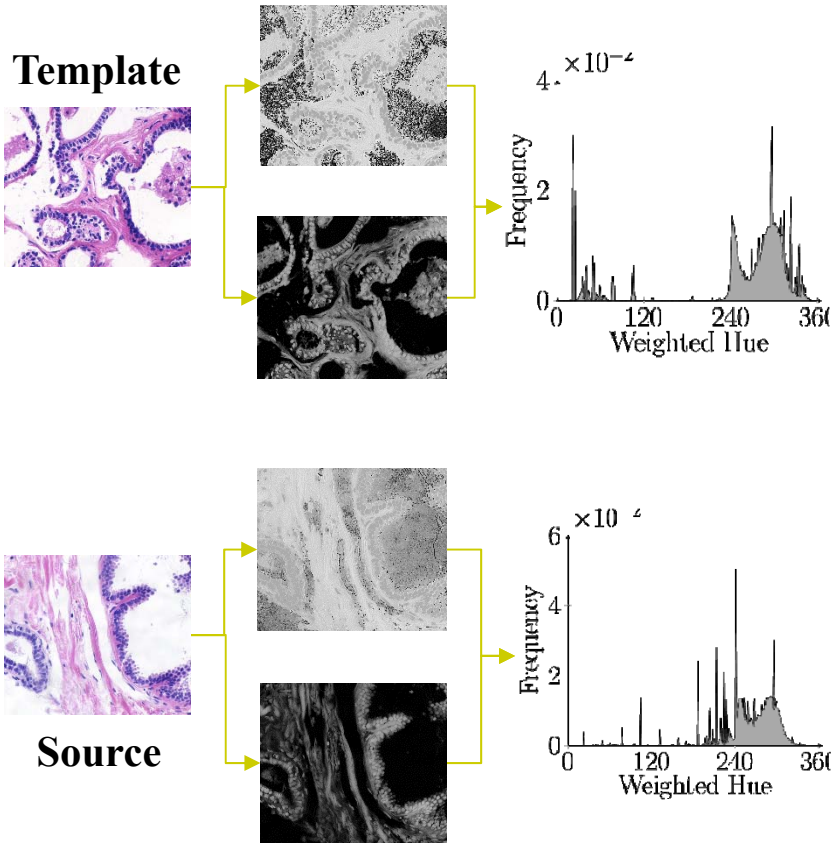

P. Maji and S. Mahapatra, "Circular Clustering in Fuzzy Approximation Spaces for Color Normalization of Histological Images", ***IEEE Transactions on Medical Imaging***, vol. 39, no. 5, pp. 1735-1745, 2020.

Color Normalization Method

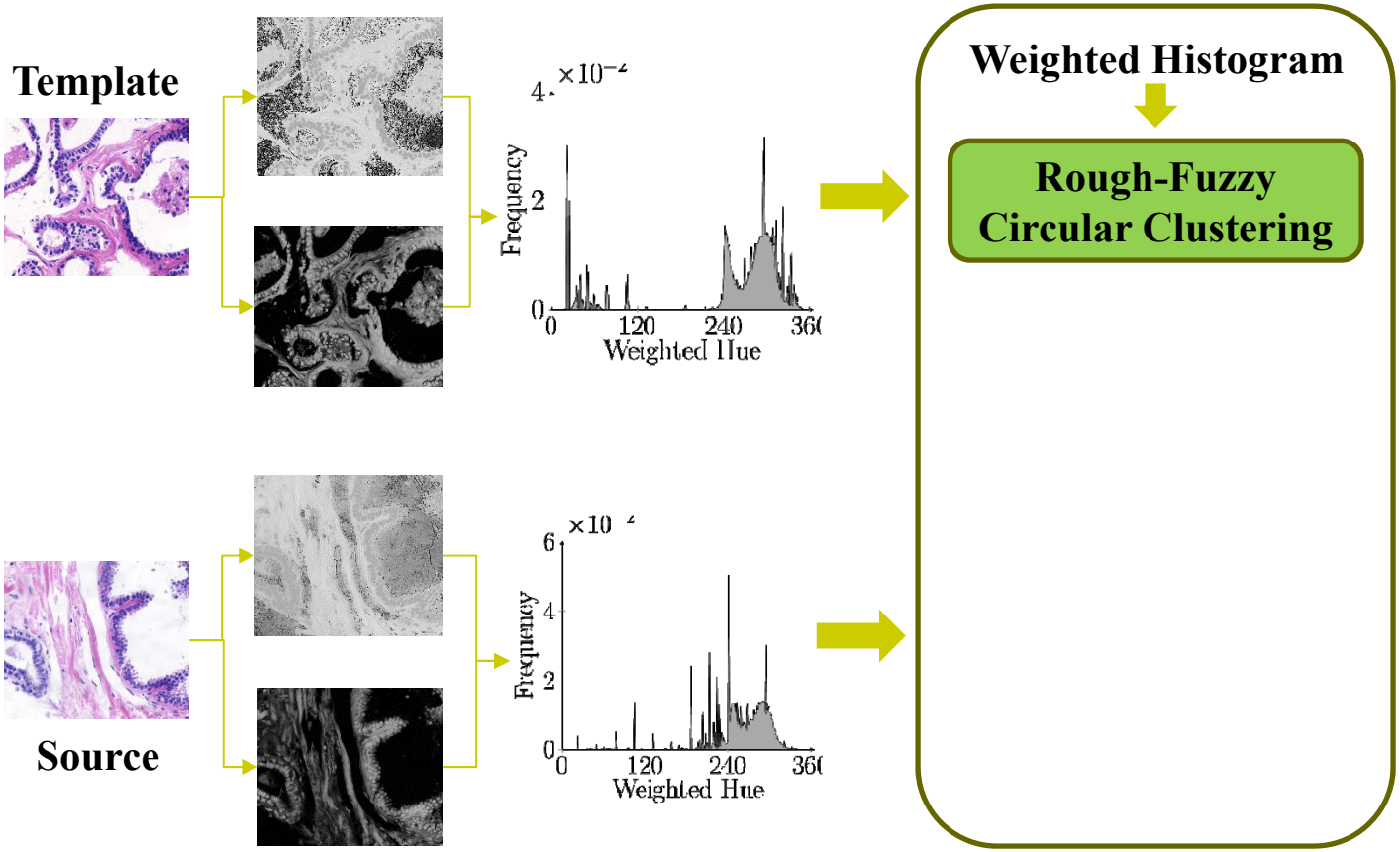

P. Maji and S. Mahapatra, "Circular Clustering in Fuzzy Approximation Spaces for Color Normalization of Histological Images", ***IEEE Transactions on Medical Imaging***, vol. 39, no. 5, pp. 1735-1745, 2020.

Color Normalization Method

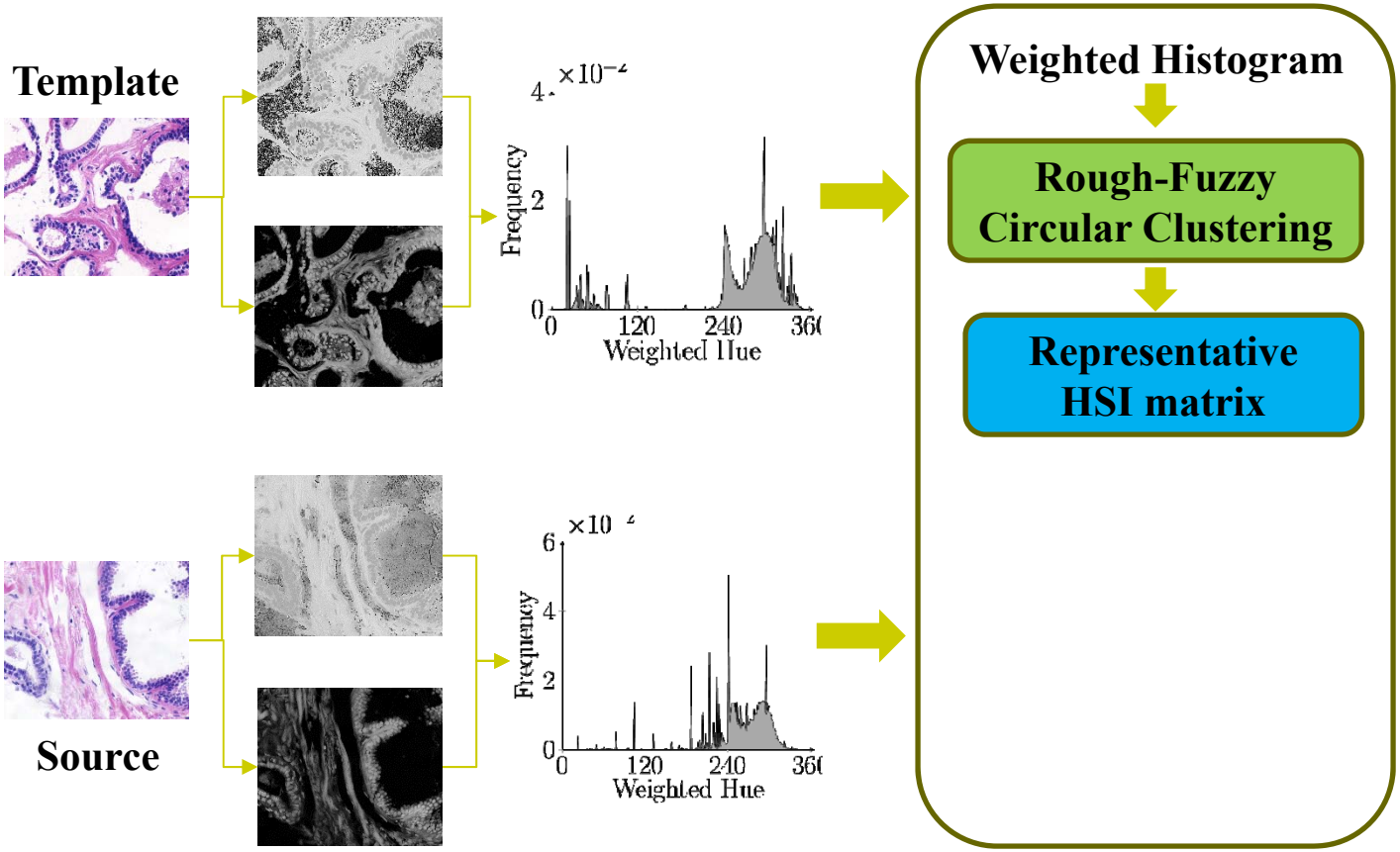

P. Maji and S. Mahapatra, "Circular Clustering in Fuzzy Approximation Spaces for Color Normalization of Histological Images", ***IEEE Transactions on Medical Imaging***, vol. 39, no. 5, pp. 1735-1745, 2020.

Color Normalization Method

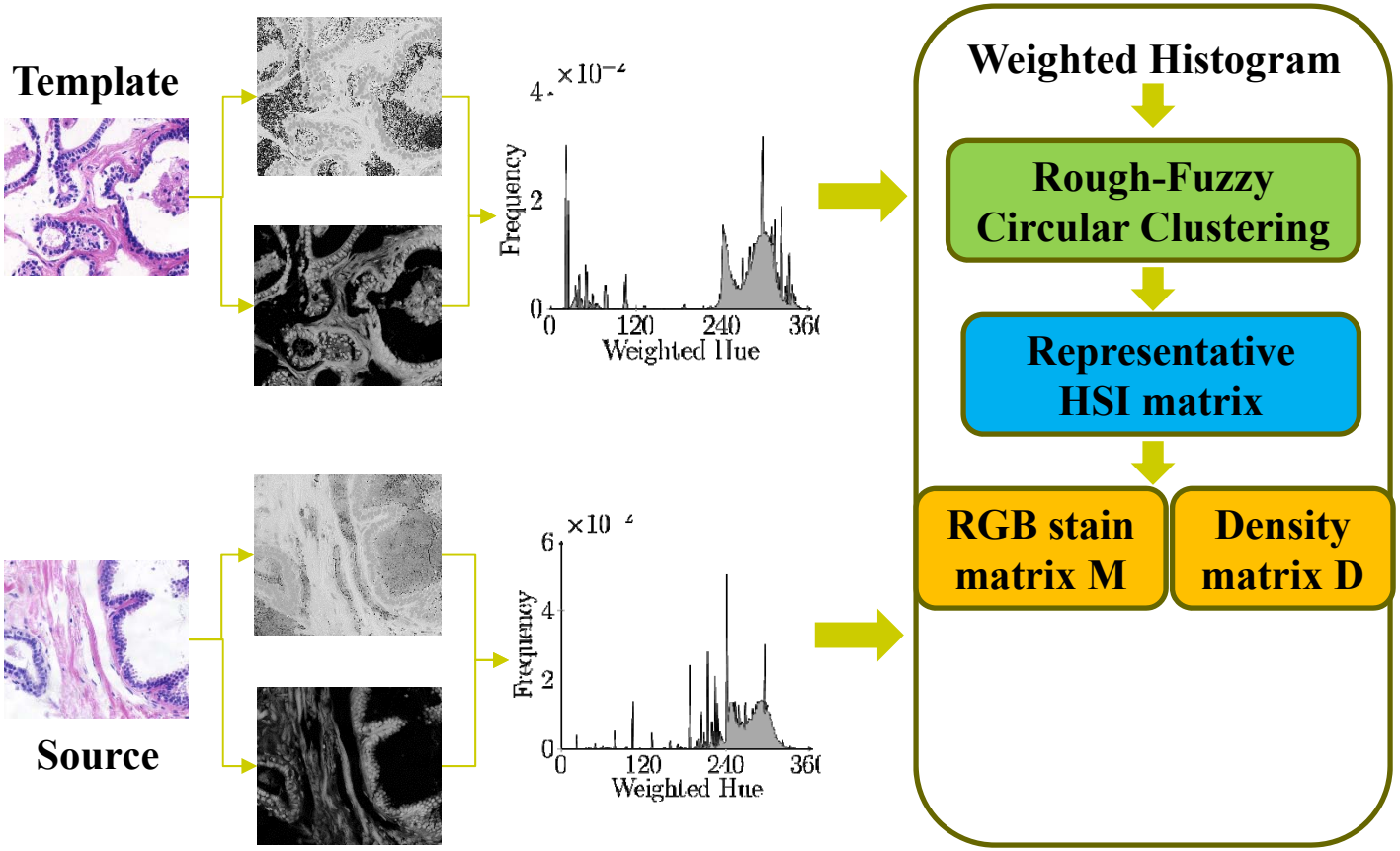

P. Maji and S. Mahapatra, "Circular Clustering in Fuzzy Approximation Spaces for Color Normalization of Histological Images", ***IEEE Transactions on Medical Imaging***, vol. 39, no. 5, pp. 1735-1745, 2020.

Color Normalization Method

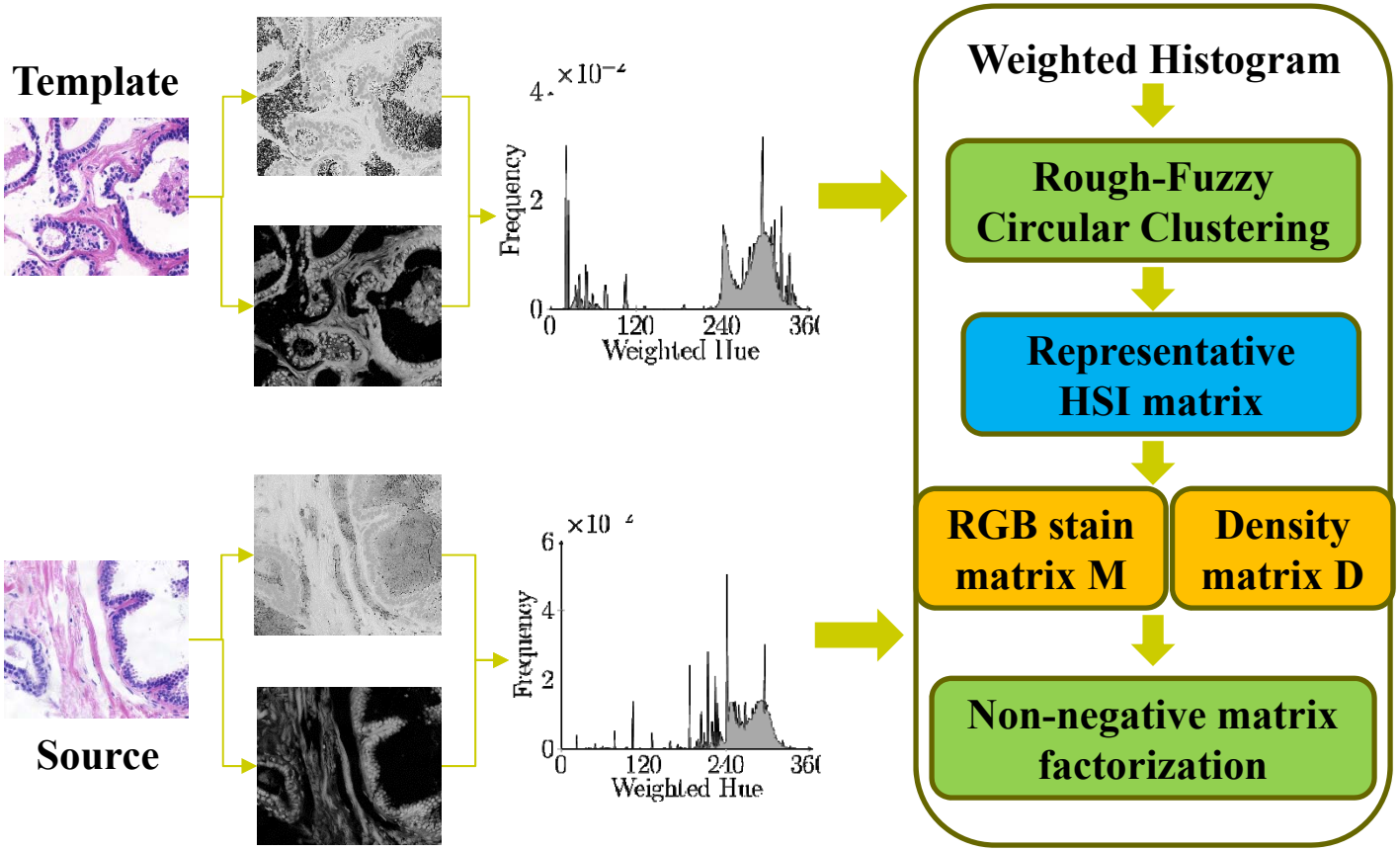

P. Maji and S. Mahapatra, "Circular Clustering in Fuzzy Approximation Spaces for Color Normalization of Histological Images", ***IEEE Transactions on Medical Imaging***, vol. 39, no. 5, pp. 1735-1745, 2020.

Color Normalization Method

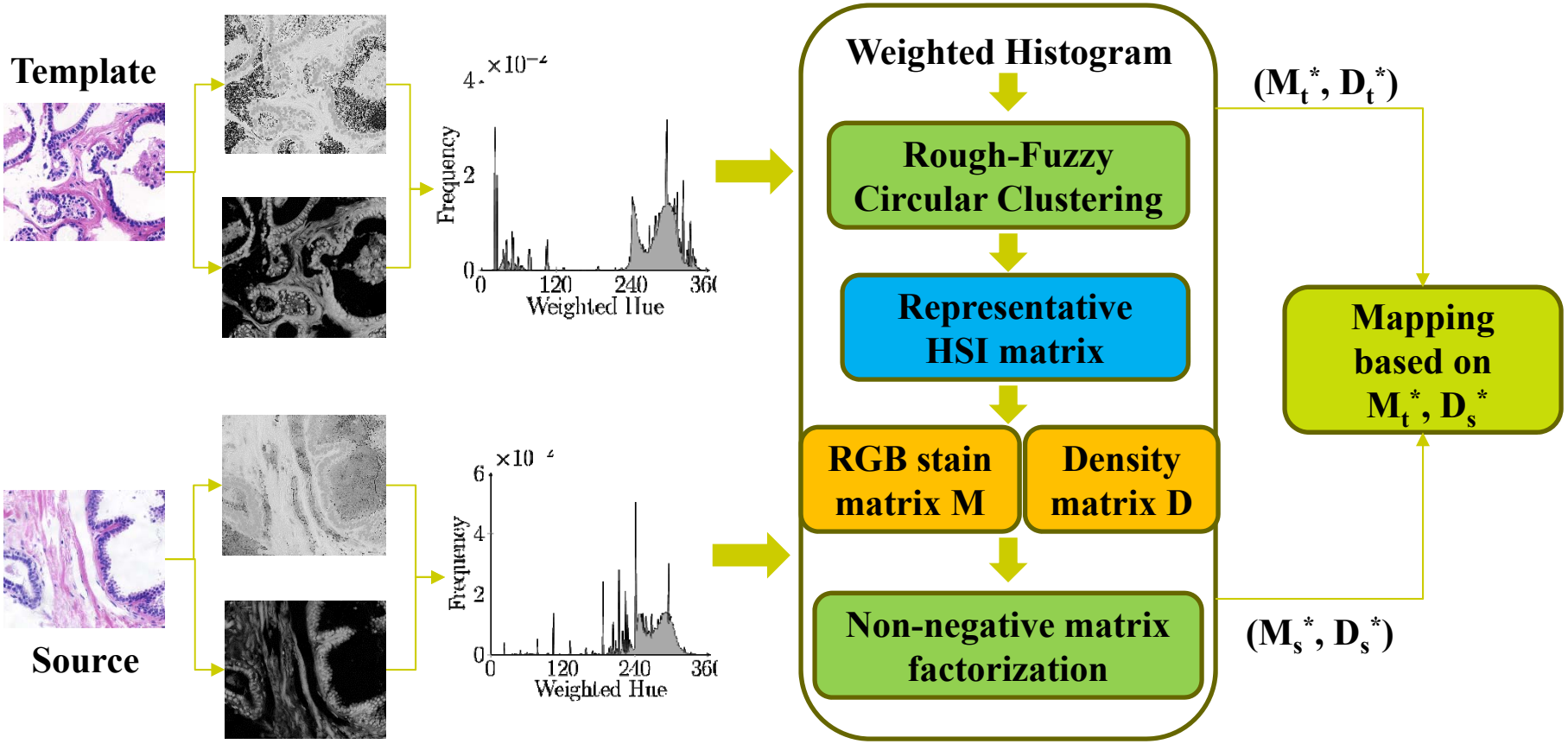

P. Maji and S. Mahapatra, "Circular Clustering in Fuzzy Approximation Spaces for Color Normalization of Histological Images", ***IEEE Transactions on Medical Imaging***, vol. 39, no. 5, pp. 1735-1745, 2020.

Color Normalization Method

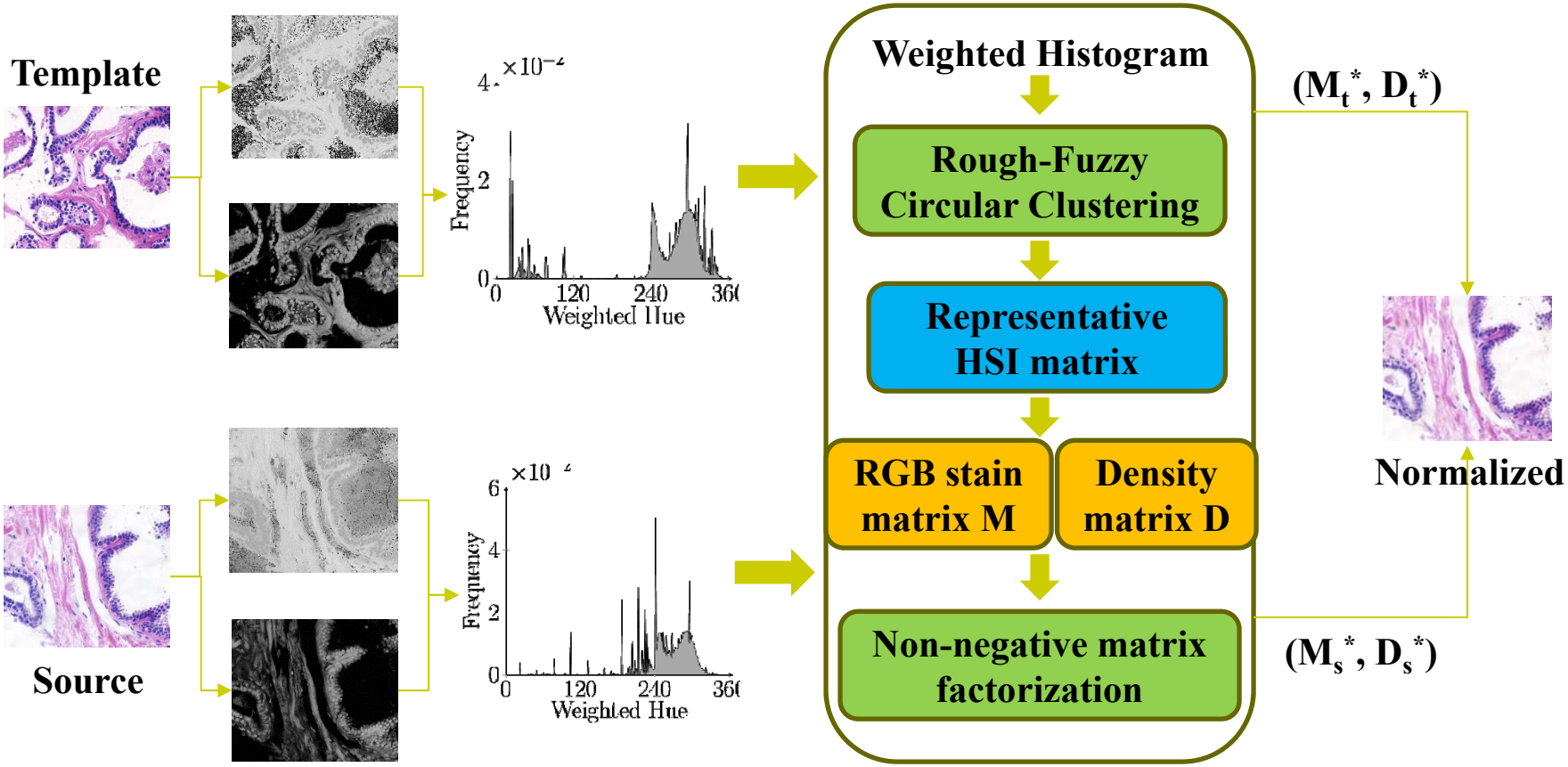

P. Maji and S. Mahapatra, "Circular Clustering in Fuzzy Approximation Spaces for Color Normalization of Histological Images", ***IEEE Transactions on Medical Imaging***, vol. 39, no. 5, pp. 1735-1745, 2020.

Description of Data Sets

- UCSB (University of California, Santa Barbara) Breast Cancer Cell Data : Total number of samples = 58
- Data specifications: hematoxylin and eosin (H&E) stained biopsy images (10 biopsy sets: 9 sets × 6 + 1 set × 4)
- Each image has a resolution of 896 × 768.
- Associated ground-truth annotation with nuclei considered as ROI.
- Images are stored in 24-bit nonlinear RGB format.
- Number of classes : Non-cancerous benign cell (32 images) and Cancerous malignant cell (26 images).

E. D. Gelasca *et al*., "Evaluation and benchmark for biological image segmentation", *IEEE International Conference on Image Processing*, 2008.

Description of Data Sets

- CMU Data (published by the bimagicLab in Carnegie Mellon University)
- Total number of samples = 3
- Data specifications: H&E stained biopsy images
- Each image has a resolution of 1280 × 1024.
- Associated stain decomposition ground-truth, separate H-stained and E-stained images.
- Images are stored in 48-bit linear RGB format.

M. T. McCann *et al*., "Algorithm and benchmark dataset for stain separation in histology images", *IEEE International Conference on Image Processing*, 2014.

Performance on UCSB Data

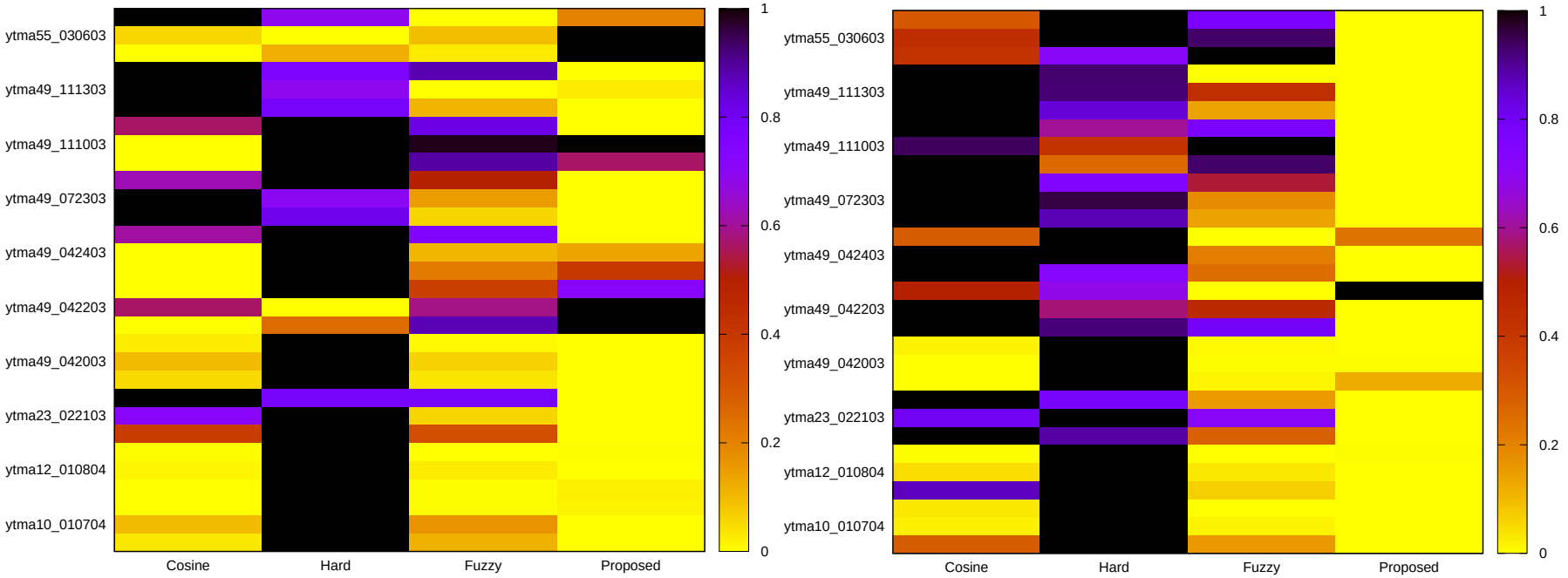

Standard deviation of estimated stain vectors of H-stain and E-stain

Performance on UCSB Data

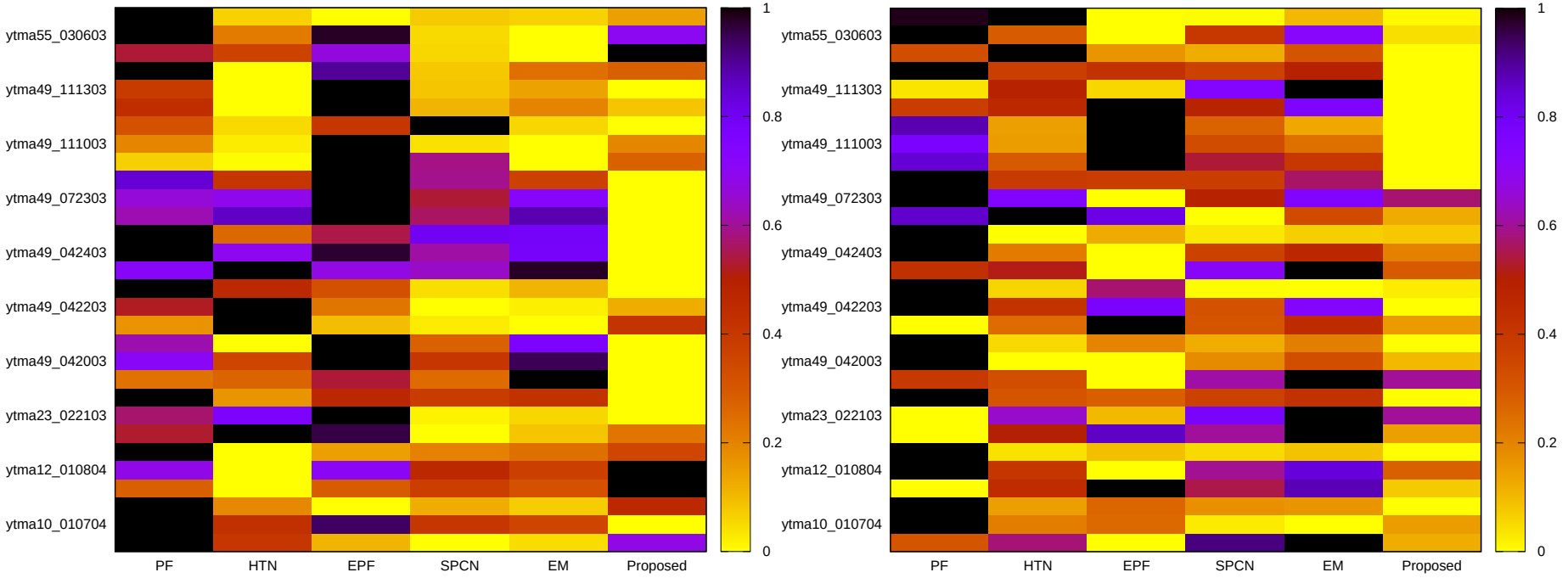

Standard deviation of estimated stain vectors of H-stain and E-stain

Performance on CMU Data

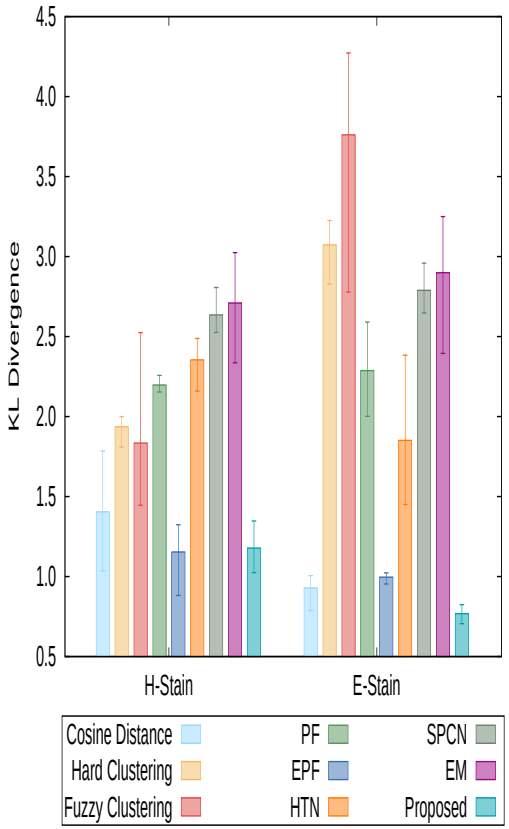

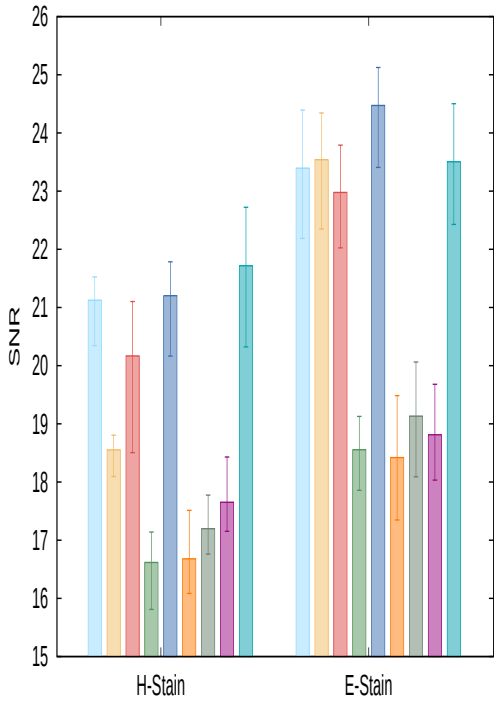

The RFCC method attains lower Kullback-Leibler (KL) divergence value w.r.t. other counterparts and existing methods except EPF

EPF performs slightly better than RFCC method in case of H-stain

Performance on CMU Data

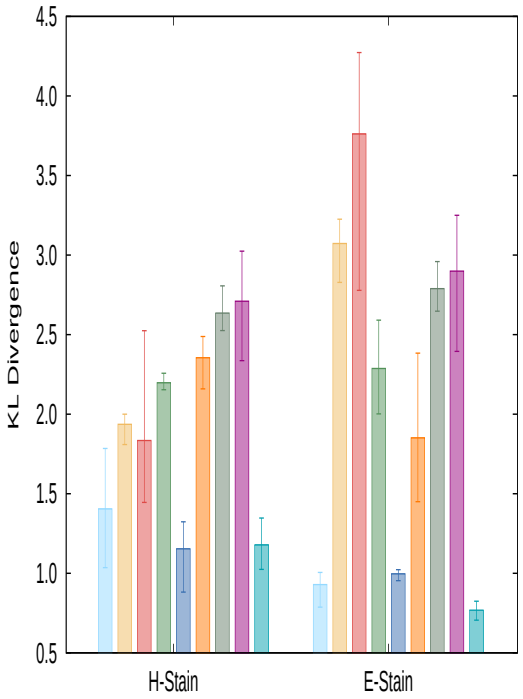

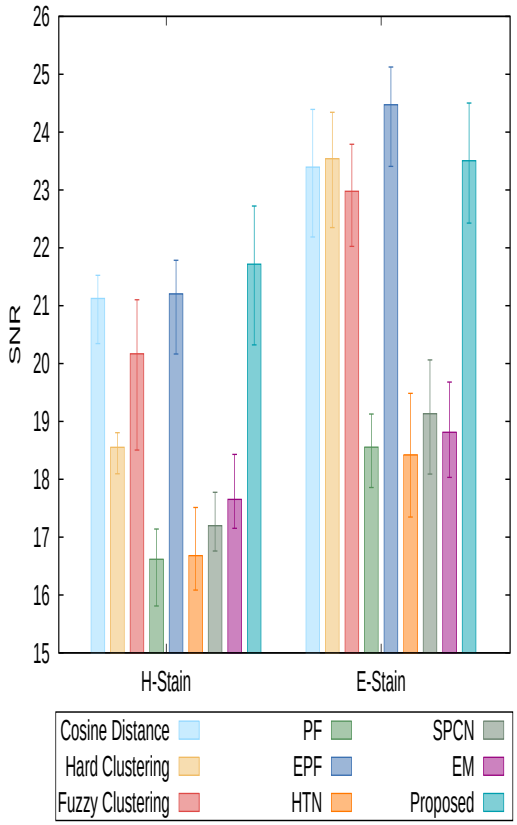

The RFCC method attains higher SNR value w.r.t. other counterparts and existing methods except EPF

EPF performs slightly better than RFCC method in case of E-stain

Performance on UCSB Data

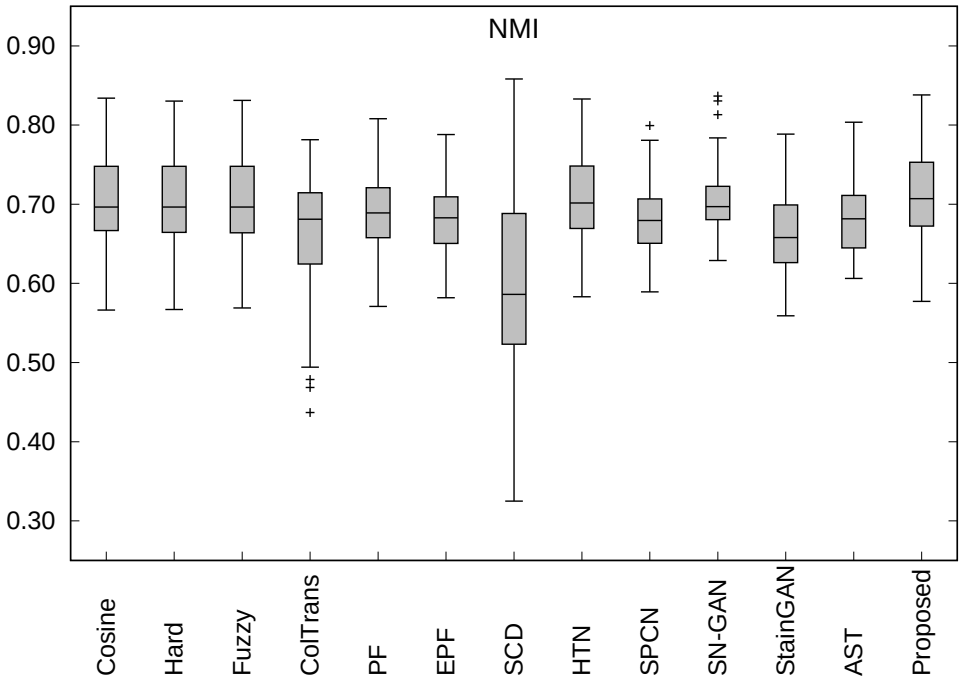

Normalized median intensity

$$\mathrm{NMI}(I) = \frac{\underset{i \in \mathrm{ROI}(I)}{\mathrm{med}} \{W(i)\}}{\underset{i \in \mathrm{ROI}(I)}{\max} \{W(i)\}}$$

It evaluates color consistency of a specific ROI within an image

sufficient??

NMI fails to capture within-biopsy color constancy information

L. G. Nyuel *et al.*, "New variants of a method of MRI scale standardization", *IEEE Transactions on Medical Imaging*, 19(2), pp. 143-150, 2000.

Quantitative Indices

Between-Image Color Constancy Index

$$\mathrm{BiCC}(I) = \frac{1}{2(|S|-1)} \times \sum_{J \neq I} \frac{\underset{i \in \mathrm{ROI}(I)}{\mathrm{med}} \{W(i)\} + \underset{j \in \mathrm{ROI}(J)}{\mathrm{med}} \{W(j)\}}{\max\{\underset{i \in \mathrm{ROI}(I)}{\max} \{W(i)\}, \underset{j \in \mathrm{ROI}(J)}{\max} \{W(j)\}\}}$$

It evaluates color consistency of ROI among images within particular same biopsy set

Within-Set Color Constancy Index

$$\mathrm{WsCC}(S) = \frac{1}{|S|} \sum_{I \in S} \mathrm{NMI}(I) \times \mathrm{BiCC}(I);$$

Overall representation of within-image and within-biopsy color consistency

Performance on UCSB Data

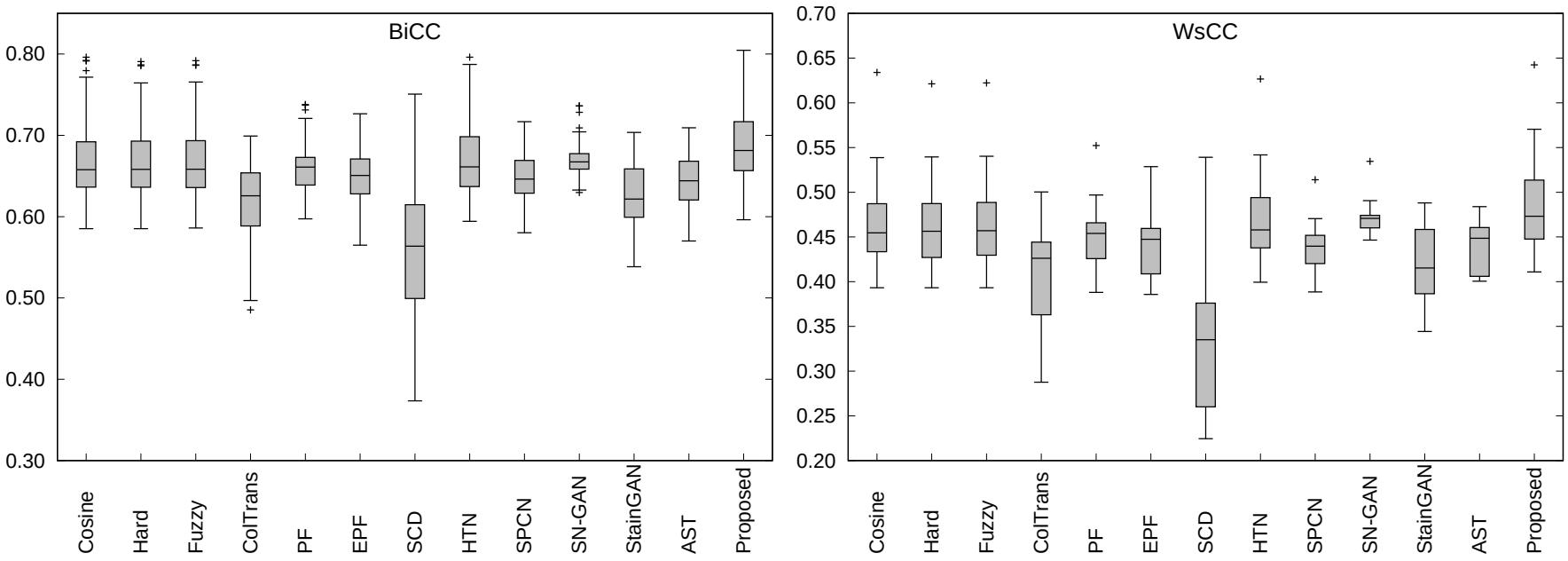

The RFCC method outperforms other existing color normalization methods as per color consistency after normalization is concerned.

Will supervised approach perform better than unsupervised approach?

TredMiL: Truncated Normal Mixture Prior Based Deep Latent Model

- It is based on least square GAN (LSGAN) [IEEE TPAMI-2019]

- It consists of four deep networks:
  - a color appearance encoder $\mathcal{E}_c$, which extracts the color appearance information,
  - a stain density encoder $\mathcal{E}_s$, which captures the information regarding amount of stains bound to biological components,
  - a decoder/generator $\mathcal{G}$, and
  - a discriminator $\mathcal{D}$.

- The networks ($\mathcal{E}_c$, $\mathcal{E}_s$, $\mathcal{G}$, $\mathcal{D}$) should be any differentiable functions so that the error values can be back-propagated during training.
  - In the current study, the networks are chosen to be convolutional neural networks.

TredMiL: Truncated Normal Mixture Prior Based Deep Latent Model

- The model assumes that the latent color appearance code (z_c) and stain density code (z_s) are independent of each other.
- A generative module and a reconstructive module are designed to capture disentangled color appearance and stain density information.
- The disentangled representation enhances the generalizability and adaptability of the model
  - loss or modification in one information does not affect the other information.
- To deal with the overlapping nature of histochemical reagents, the TredMiL assumes that the latent color appearance code, extracted through the color appearance encoder, is sampled from a mixture of truncated normal distributions.

TredMiL: Truncated Normal Mixture Prior Based Deep Latent Model

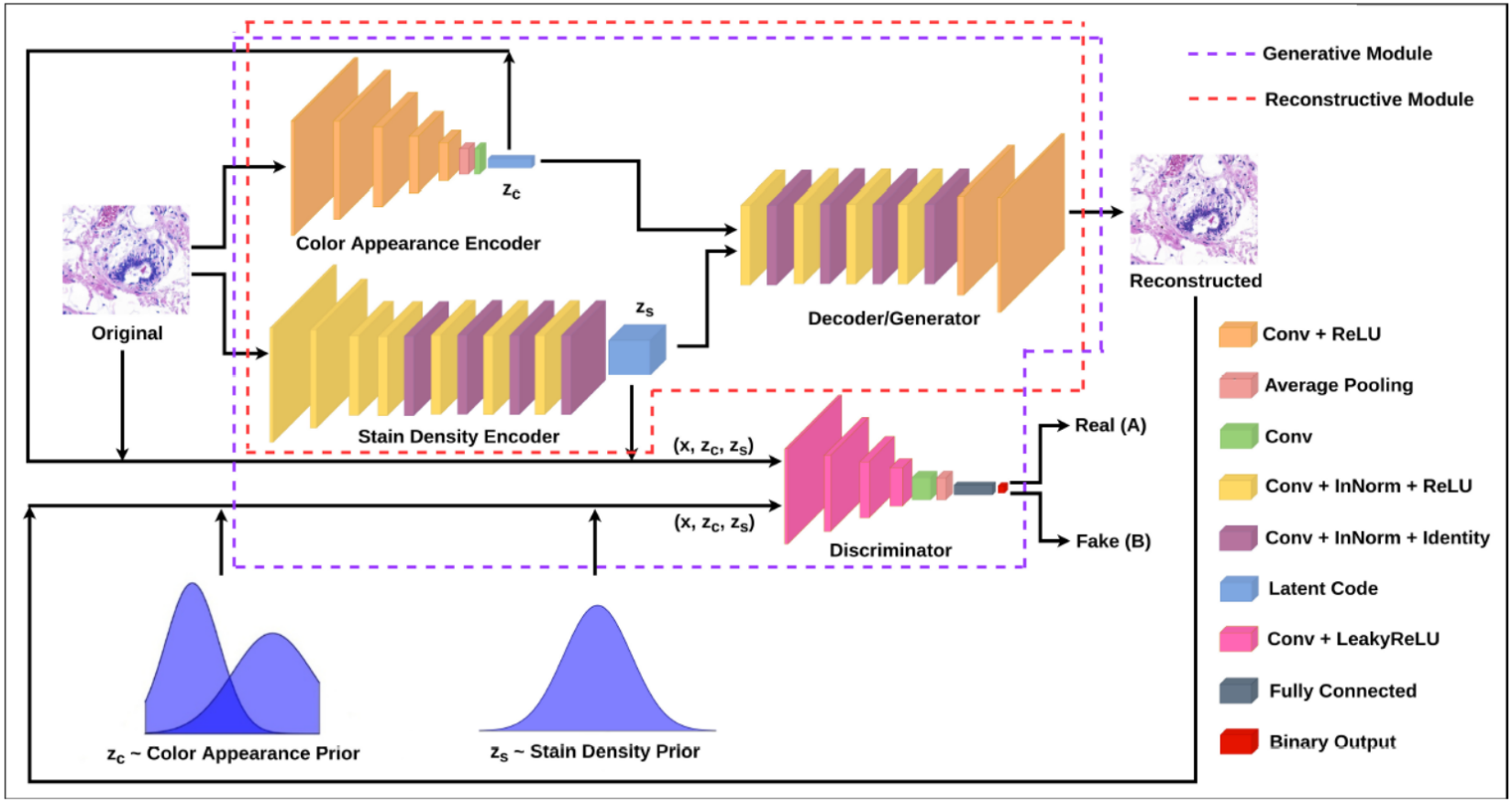

'Conv' means convolutional layer, 'ReLU' denotes rectified linear unit, 'InNorm' represents instance normalization, 'Identity' means identity function, i.e., $f(x) = x$, 'LeakyReLU' denotes leaky rectified linear unit.

TredMiL: Truncated Normal Mixture Prior Based Deep Latent Model

- Each training set image $\boldsymbol{x}$ is fed simultaneously into
  - the color appearance encoder $\mathcal{E}_c(\boldsymbol{x}; \boldsymbol{\theta}_{Ec})$ and
  - the stain density encoder $\mathcal{E}_s(\boldsymbol{x}; \boldsymbol{\theta}_{Es})$,
- which eventually output
  - the latent color appearance code $\boldsymbol{z}_c$ and
  - latent stain density representation $\boldsymbol{z}_s$, respectively.
- Both the latent representations, $\boldsymbol{z}_c$ and $\boldsymbol{z}_s$, are fed into the decoder /generator as inputs, which generates the reconstructed image.
- The discriminator $\mathcal{D}$ takes inputs in the form of triplets $(\boldsymbol{x}; \boldsymbol{z}_c; \boldsymbol{z}_s)$ and discriminates real encoding from the generated/fake encoding.

S. Mahapatra and P. Maji, Truncated Normal Mixture Prior Based Deep Latent Model for Color Normalization of Histology Images, ***IEEE Transactions on Medical Imaging***, 42(6), pp. 1746--1757, June 2023.

TredMiL: Objective Function

- The adversarial objective term, attributed by the generative module, is framed as follows:

$$J_{\text{adv}} = J_{\text{G}}(\mathcal{D}) + J_{\text{G}}(\mathcal{G})$$

- The objective functions, corresponding to the generative module, are given as follows:

$$J_{\text{G}}(\mathcal{D}) = \min_{\mathcal{D}} J_1(\mathcal{E}_c, \mathcal{E}_s, \mathcal{G}, \mathcal{D}),$$

$$J_1(\mathcal{E}_c, \mathcal{E}_s, \mathcal{G}, \mathcal{D}) = \underbrace{E_{x\sim P_X(x)} E_{z_c\sim P_{\mathcal{E}_c}(z_c|x)} E_{z_s\sim P_{\mathcal{E}_s}(z_s|x)} (A - \mathcal{D}[x, z_c, z_s])^2}_{R}$$
$$+ \underbrace{E_{z_c\sim P_{z_c}(z_c)} E_{z_s\sim P_{z_s}(z_s)} E_{x\sim P_{\mathcal{G}}(x|z_c,z_s)} (B - \mathcal{D}[x, z_c, z_s])^2}_{G}$$

- A and B denote the labels, assigned by discriminator $\mathcal{D}$, to designate real and generated/fake encoding, respectively.

TredMiL: Objective Function

- Similarly, $$J_{\mathrm{G}}(\mathcal{G}) = \min_{\mathcal{G}} J_2(\mathcal{E}_c, \mathcal{E}_s, \mathcal{G}, \mathcal{D}),$$

$$J_2(\mathcal{E}_c, \mathcal{E}_s, \mathcal{G}, \mathcal{D}) = E_{z_c \sim P_{z_c}(z_c)} E_{z_s \sim P_{z_s}(z_s)} E_{x \sim P_{\mathcal{G}}(x|z_c, z_s)} (C - \mathcal{D}[x, z_c, z_s])^2$$

- C represents the label, assigned by discriminator $\mathcal{D}$ to designate generated/fake encoding, as desired by generator $\mathcal{G}$.

- The reconstruction objective to be minimized is as follows:

$$J_{\mathrm{rec}} = \underbrace{-E_{Q(z_c,z_s)}[\log P_{\mathcal{G}}(x \mid z_c, z_s)]}_{L_R} - E_{Q(z_c,z_s)}[\log Q(z_c, z_s)] + \underbrace{D_{KL}[Q(z_c) \mid\mid P_{z_c}(z_c)]}_{R_1} + \underbrace{D_{KL}[Q(z_s) \mid\mid P_{z_s}(z_s)]}_{R_2},$$

- where L_R represents the reconstruction loss, R_1 and R_2 denote the regularization terms corresponding to color appearance code z_c and stain density code z_s, respectively, and D_{KL} is the KL divergence.

TredMiL: Training

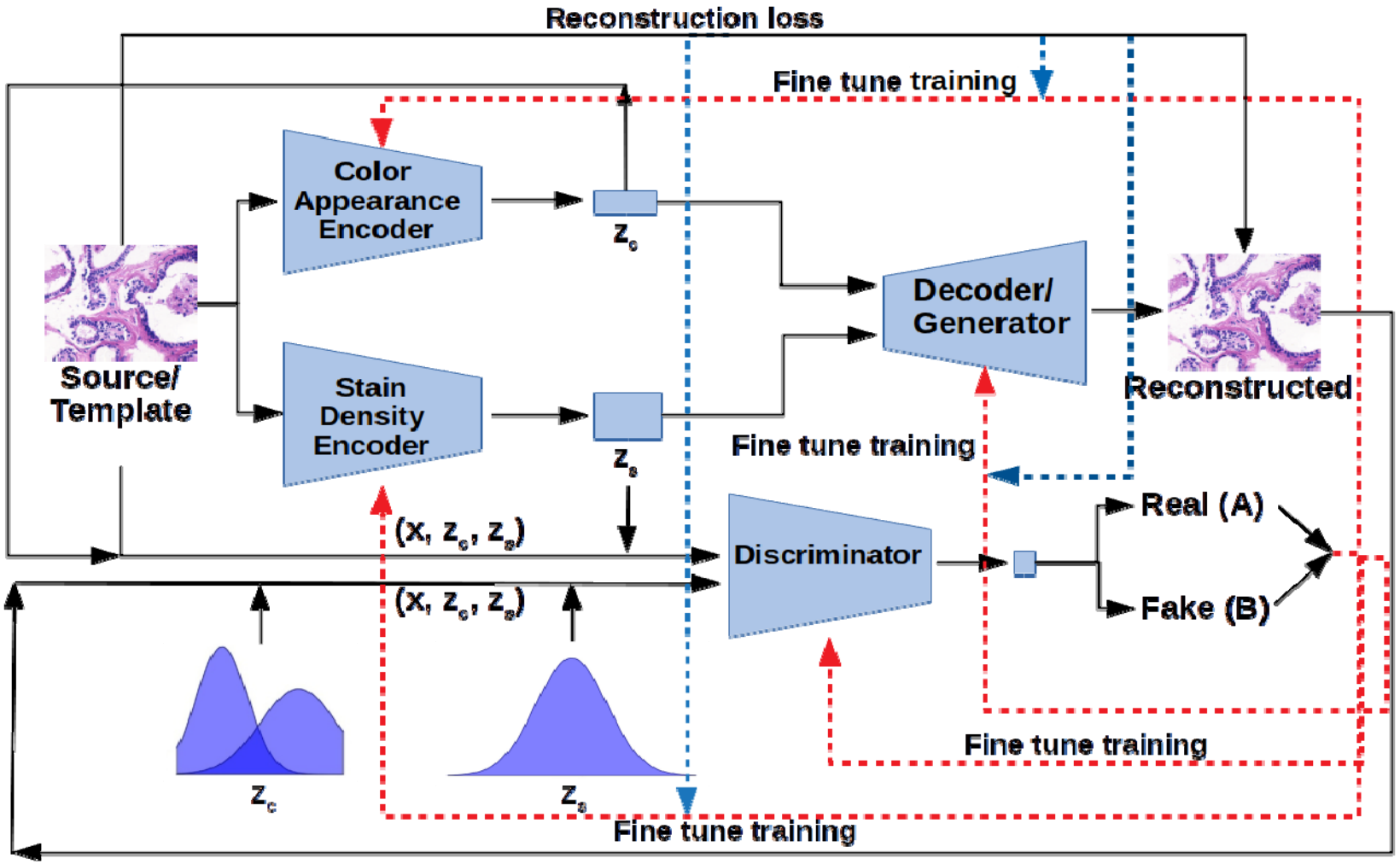

TredMiL: Color Normalization

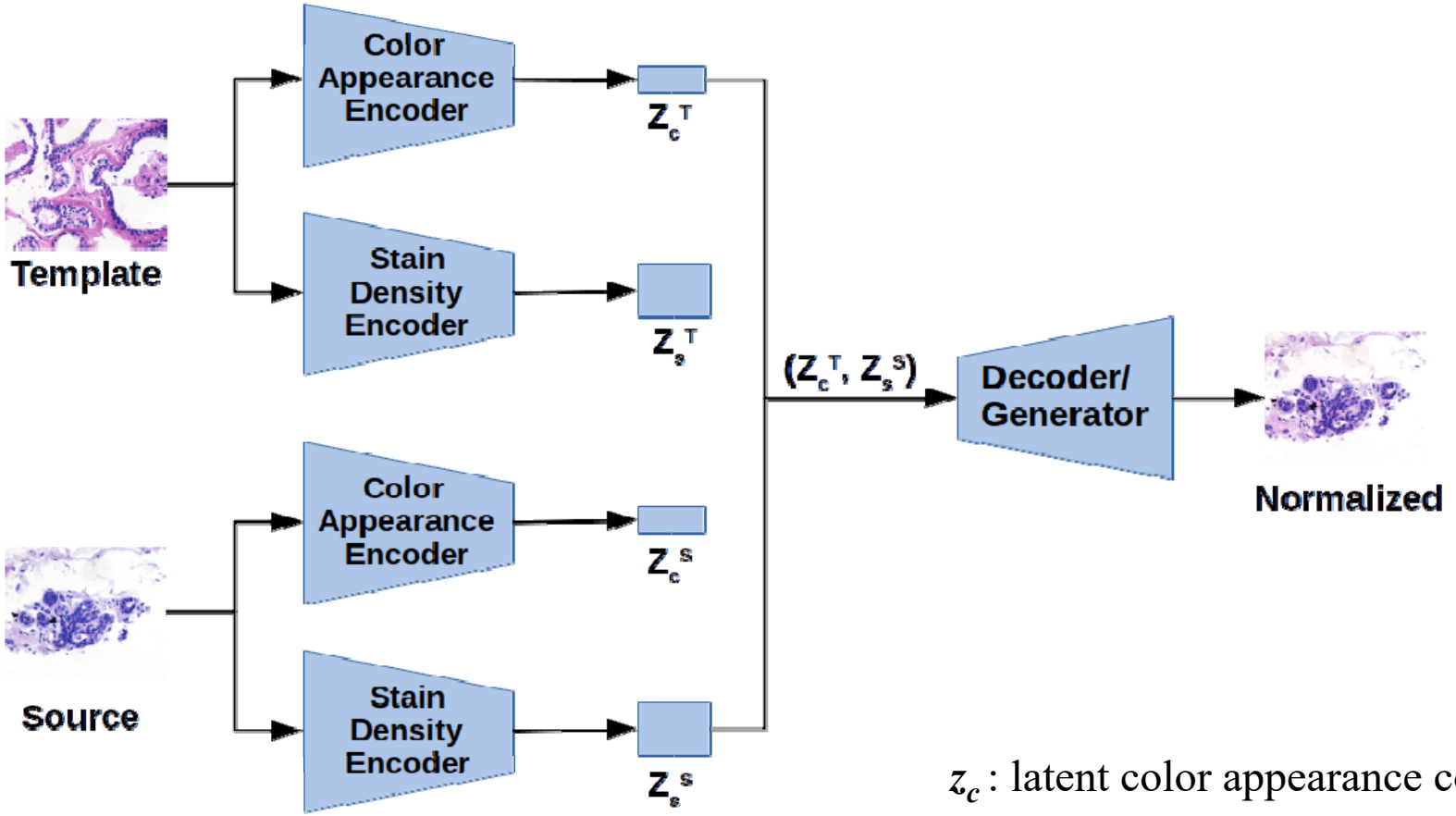

z_c : latent color appearance code

z_s : latent stain density code

TredMiL in Presence of Dust

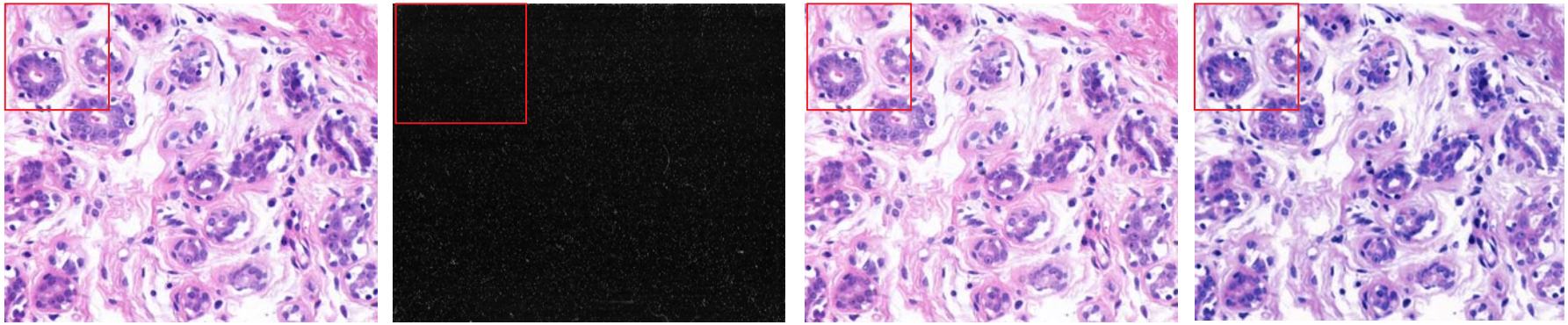

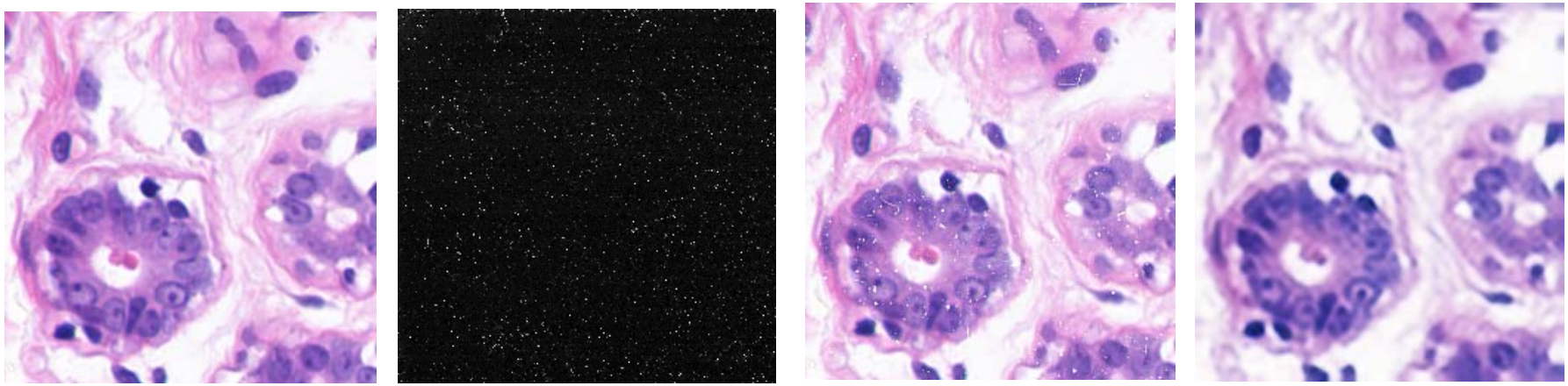

Original | Dust film | Dust added | Reconstructed

TredMiL: Effect of Fading

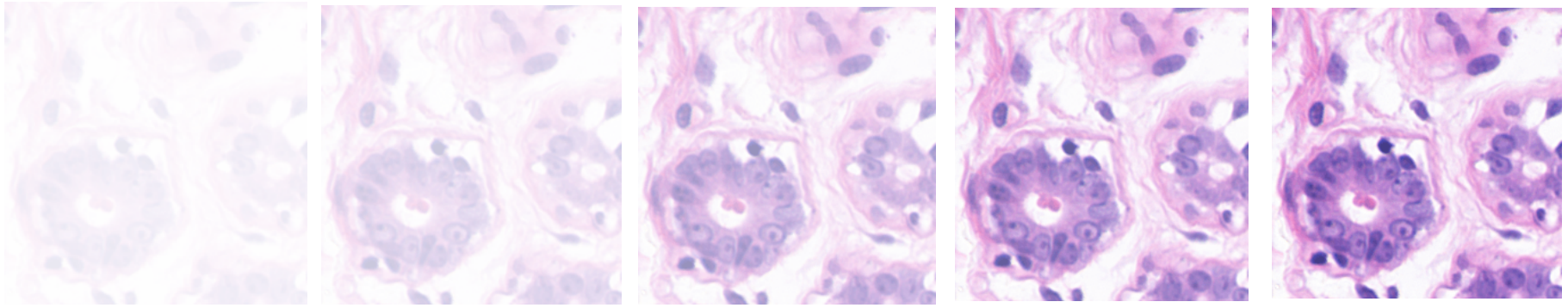

Opacity=10 Opacity=25 Opacity=50 Opacity=75 Opacity=90

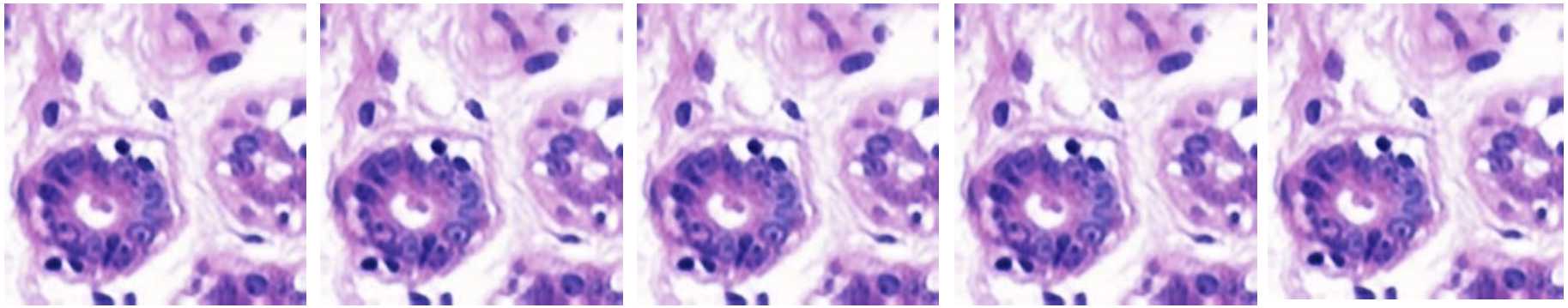

Color Normalization on Nuclei Segmentation

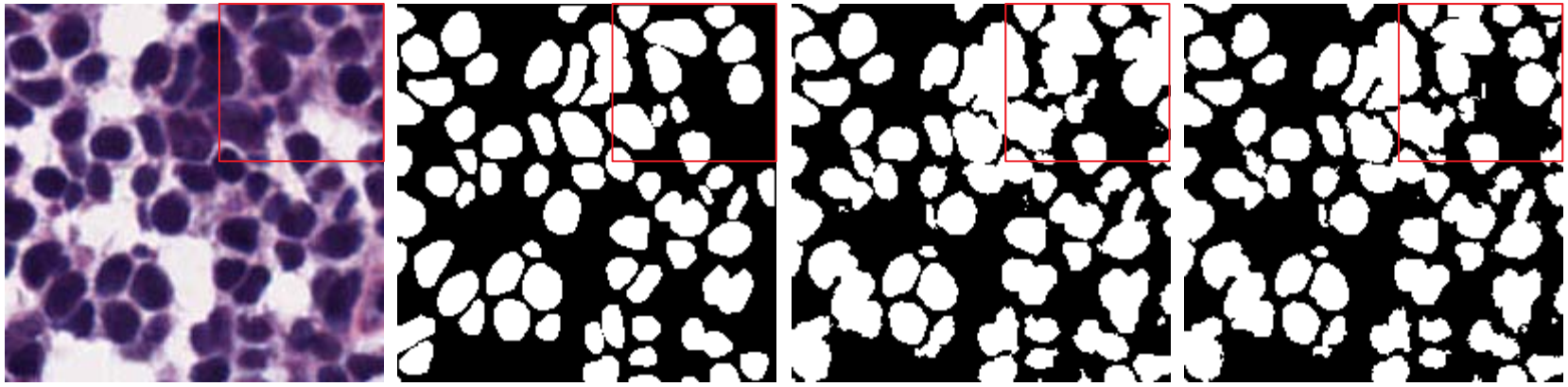

Original | Ground-truth | Before normalization | After normalization

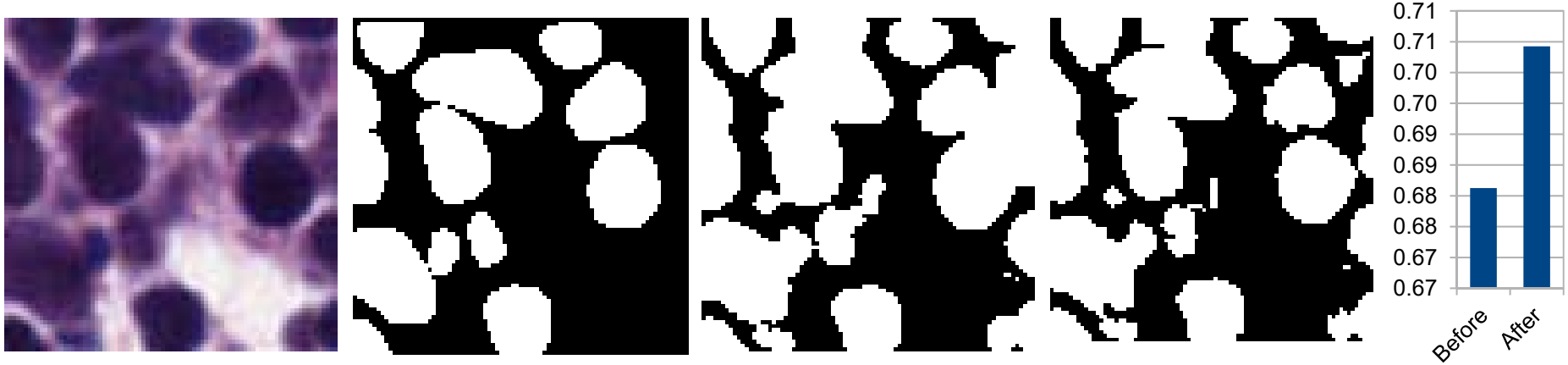

N. Kumar et al., "A Dataset and a Technique for Generalized Nuclear Segmentation for Computational Pathology", ***IEEE Transactions on Medical Imaging***, 36(7), pp. 1550-1560, 2017.

Stain Vector Estimation

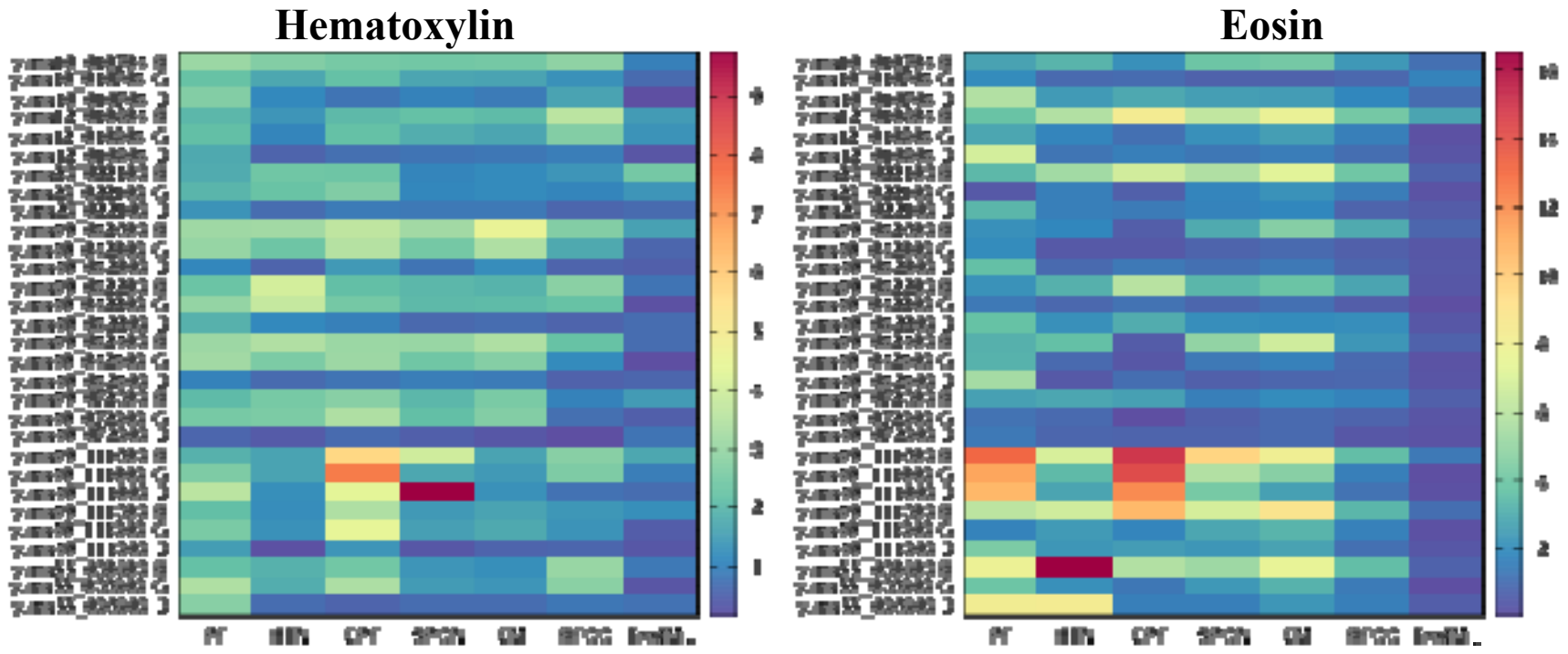

Standard deviation of estimated stain vectors of H-stain and E-stain

PF for Stain Separation

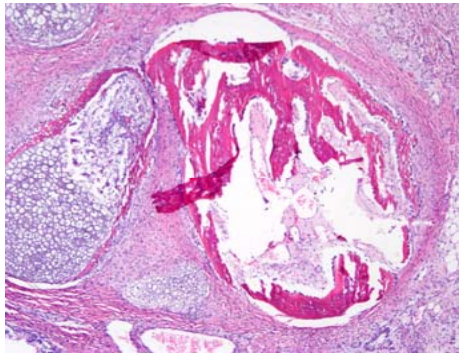

H&E Stained Image

H-Stain

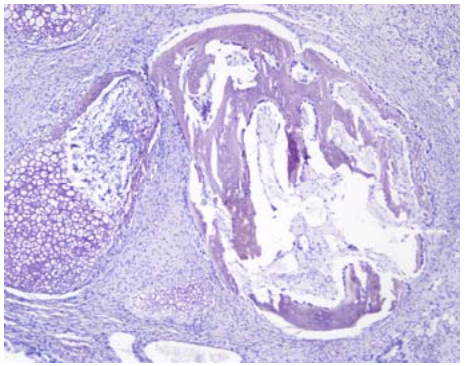

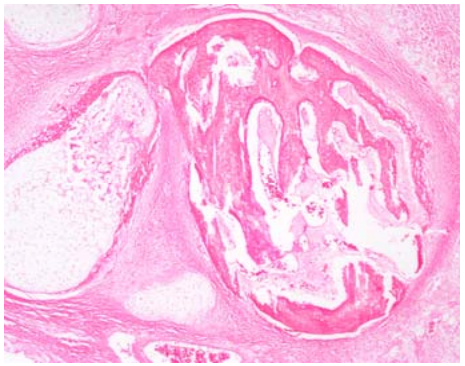

E-Stain

KL Div: 2.15, SNR: 15.81

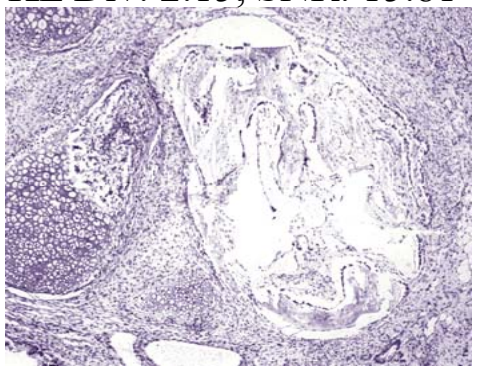

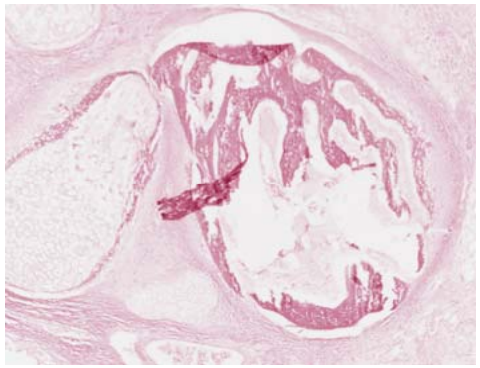

KL Div: 2.00, SNR: 17.86

M. Macenko, M. Niethammer, J. Marron, D. Borland, J. T. Wooseley, X. Guan, C. Schmitt, and N. E. Thomas, "A Method for Normalizing Histology Slides for Quantitative Analysis", ***IEEE International Symposium on Biomedical Imaging: From Nano to Macro***, pp. 1107-1110, 2009.

EPF for Stain Separation

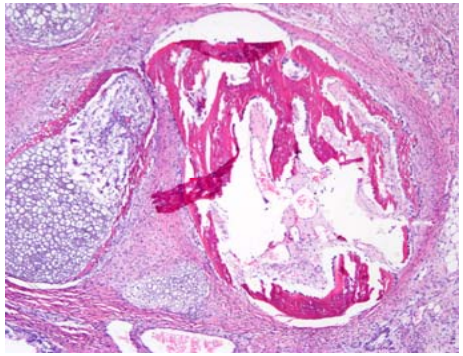

H&E Stained Image

H-Stain

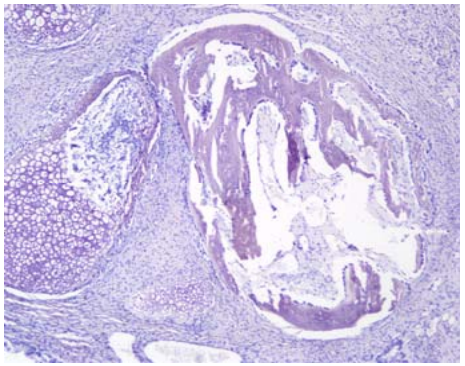

KL Div: 1.25, SNR: 20.16

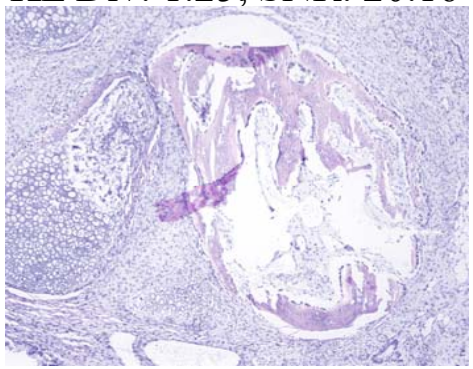

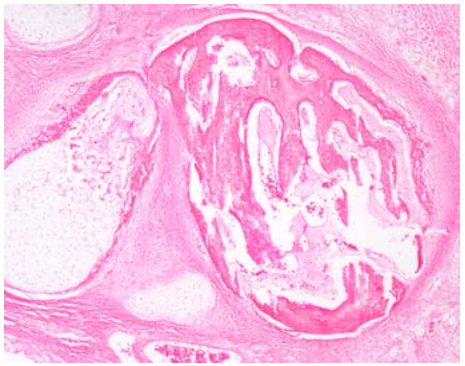

E-Stain

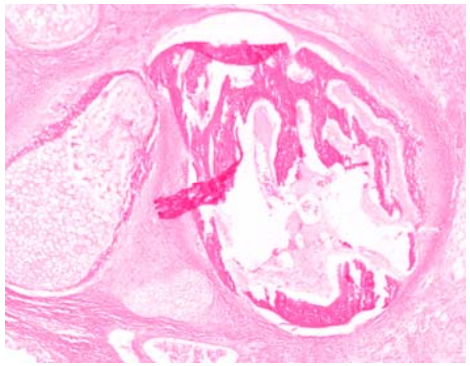

KL Div: 1.01, SNR: 23.41

M. T. McCann et al., "Algorithm and Benchmark Dataset for Stain Separation in Histology Images", ***IEEE International Conference on Image Processing***, pp. 3953-3957, 2014.

HTN for Stain Separation

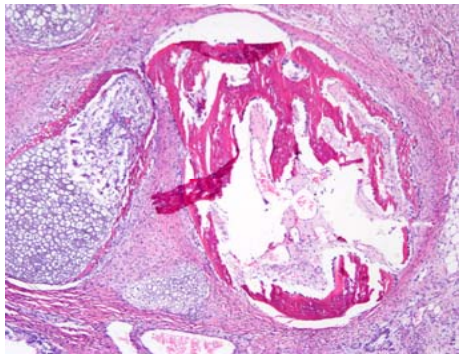

H&E Stained Image

H-Stain

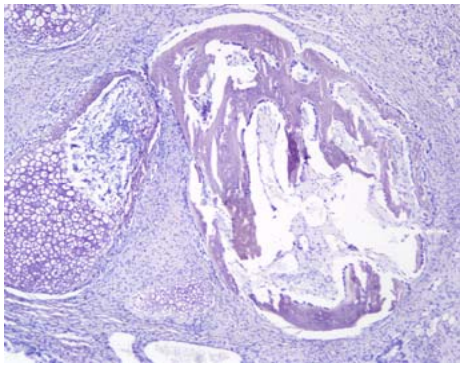

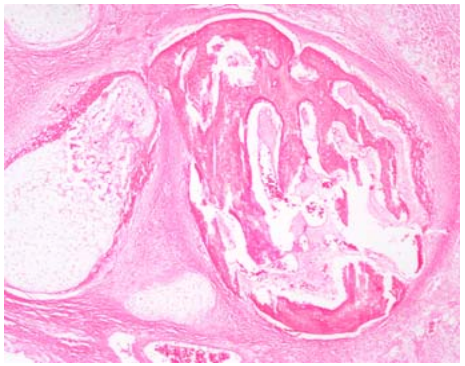

E-Stain

KL Div: 2.42, SNR: 16.09

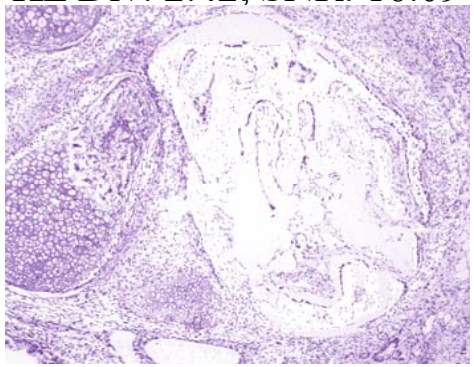

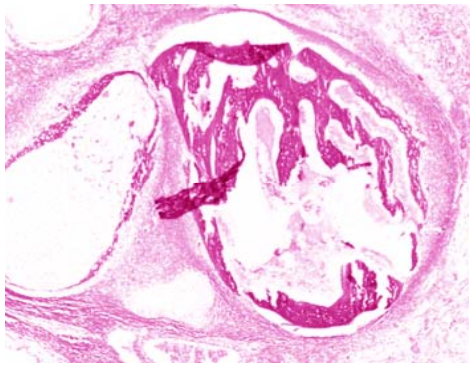

KL Div: 2.38, SNR: 17.35

X. Li and K. N. Plataniotis, "A Complete Color Normalization Approach to Histopathology Images Using Color Cues Computed From Saturation-Weighted Statistics", ***IEEE Transactions on Biomedical Engineering***, 62(7), pp. 1862-1873, 2015.

SPCN for Stain Separation

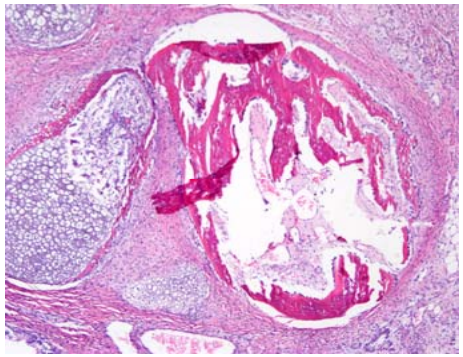

H&E Stained Image

H-Stain

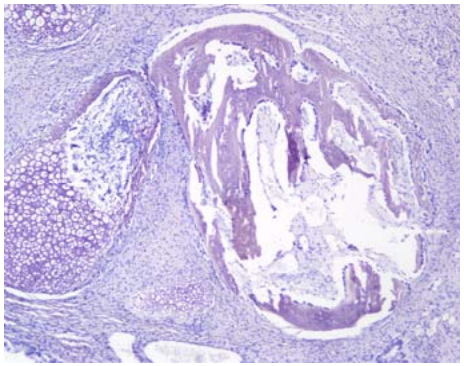

KL Div: 2.57, SNR: 16.76

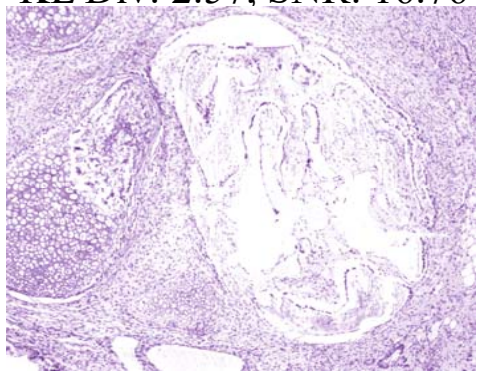

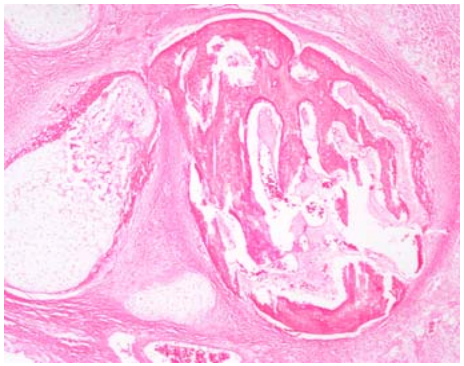

E-Stain

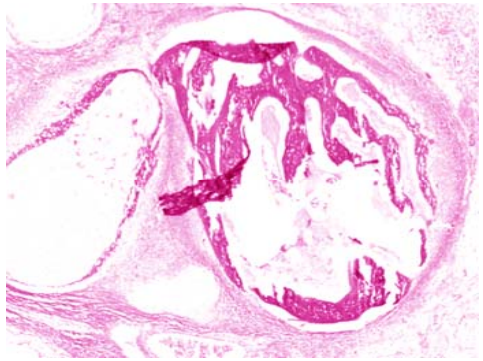

KL Div: 2.96, SNR: 18.09

A.Vahadane et al., "Structure-Preserving Color Normalization and Sparse Stain Separation for Histological Images", ***IEEE Transactions on Medical Imaging***, 35(8), pp. 1962-1971, 2016.

EM for Stain Separation

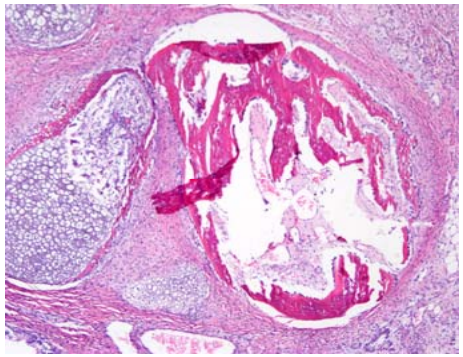

H&E Stained Image

H-Stain

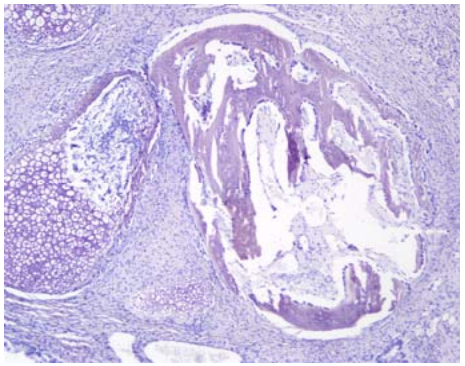

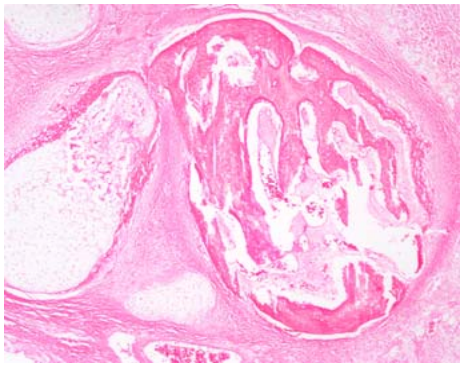

E-Stain

KL Div: 2.34, SNR: 17.15

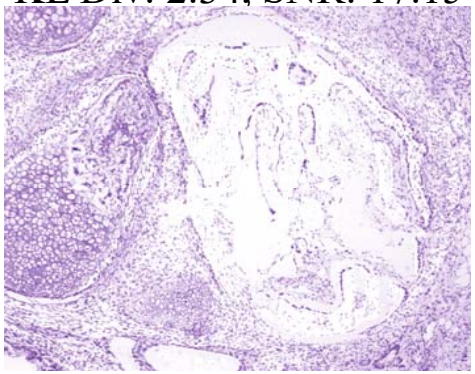

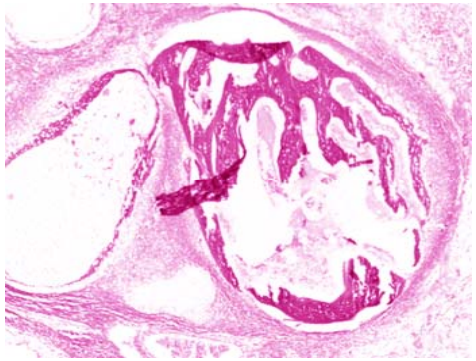

KL Div: 2.39, SNR: 18.03

X. Li and K. N. Plataniotis, "Circular Mixture Modeling of Color Distribution for Blind Stain Separation in Pathology Images", ***IEEE Journal on Biomedical and Health Informatics***, 21(1), pp. 150-161, 2017.

RFCC for Stain Separation

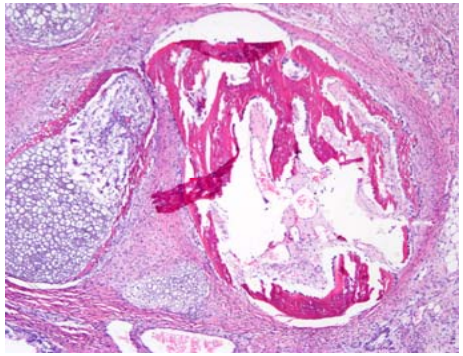

H&E Stained Image

H-Stain

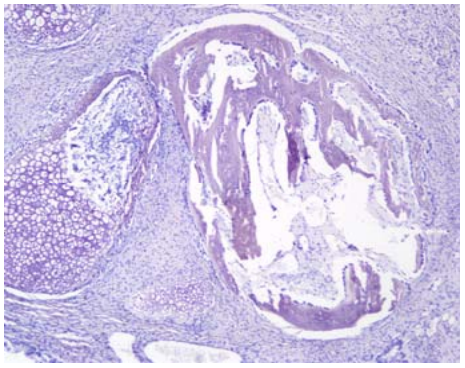

KL Div: 1.16, SNR: 20.32

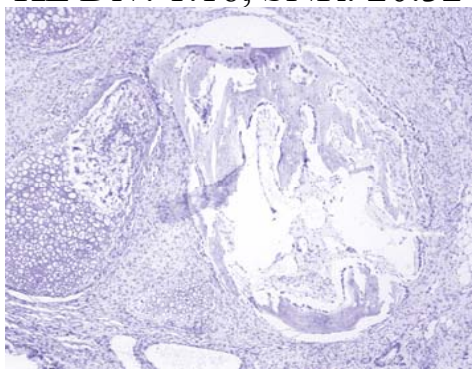

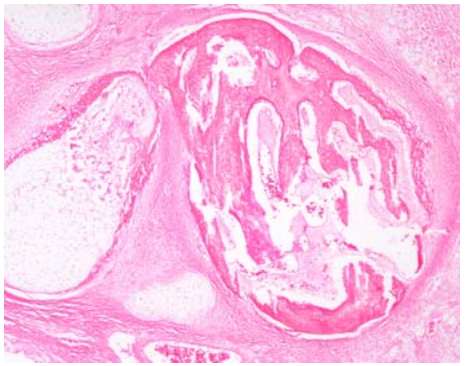

E-Stain

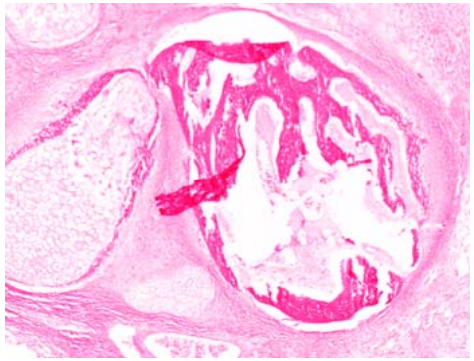

KL Div: 0.82, SNR: 22.43

P. Maji and S. Mahapatra, "Circular Clustering in Fuzzy Approximation Spaces for Color Normalization of Histological Images", ***IEEE Transactions on Medical Imaging***, pp. 1735-1745, vol. 39, no. 5, 2020.

TredMiL for Stain Separation

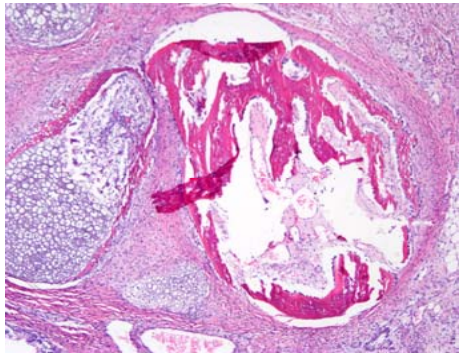

H&E Stained Image

H-Stain

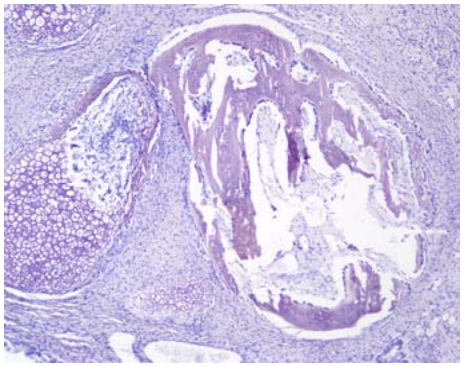

KL Div: 1.01, SNR: 22.25

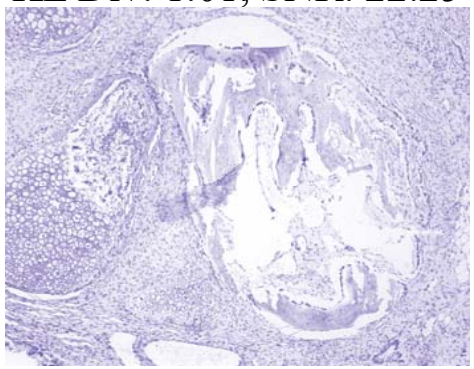

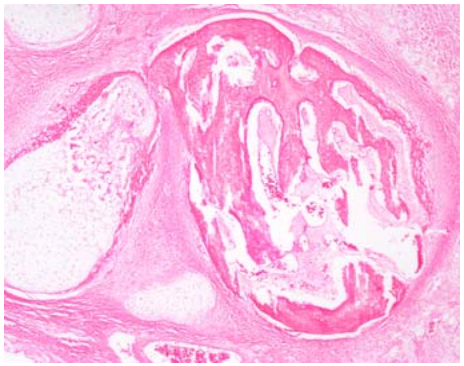

E-Stain

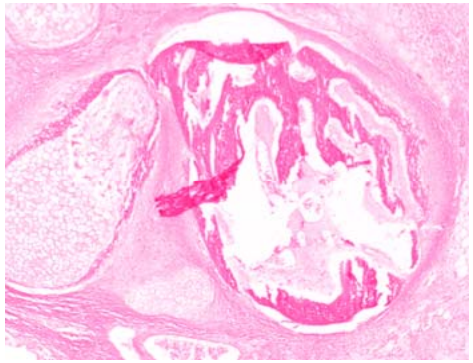

KL Div: 0.60, SNR: 25.53

S. Mahapatra and P. Maji, "Truncated Normal Mixture Prior Based Deep Latent Model for Color Normalization of Histology Images", ***IEEE Transactions on Medical Imaging***, 42(6), pp. 1746--1757, June 2023.

Stain Separation

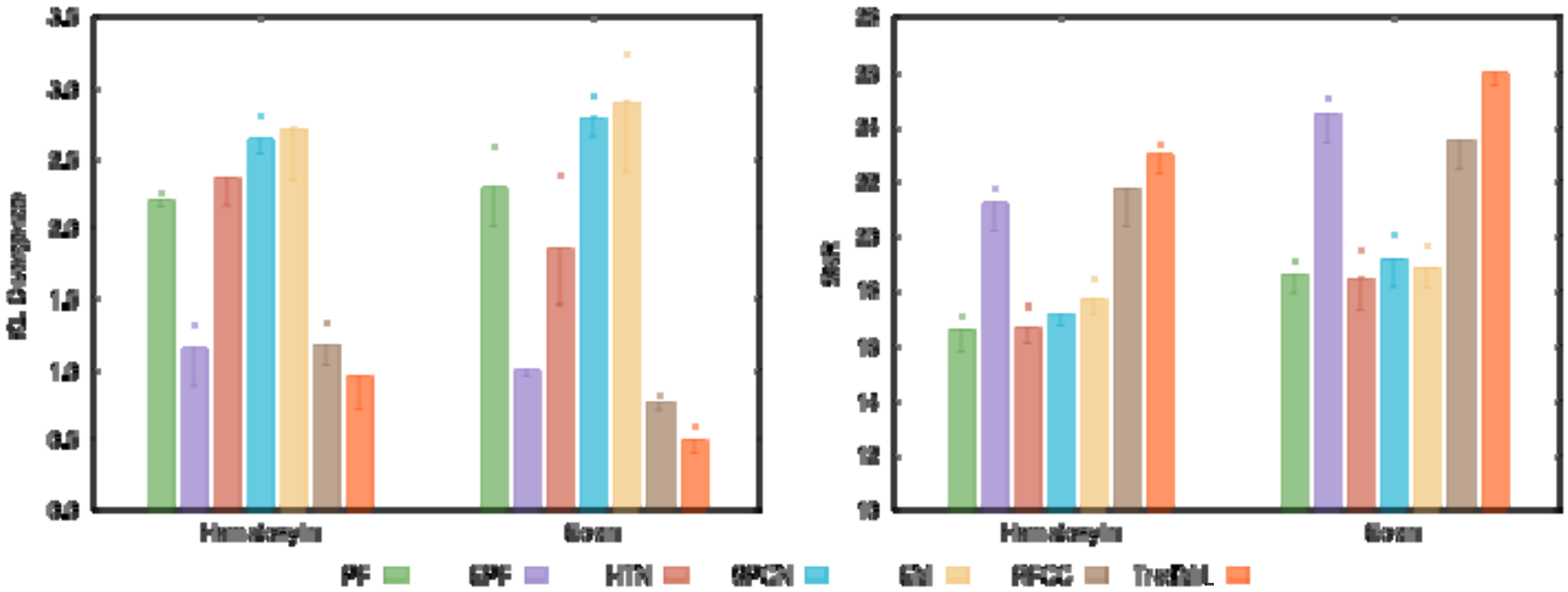

Only RFCC, TredMiL and EPF can extract intrinsic structures of biological components, highlighted by H-stain and E-stain

But, unlike EPF, the RFCC and TredMiL are applicable to cases with more than 2 stains

Qualitative Analysis: Color Normalization

Source

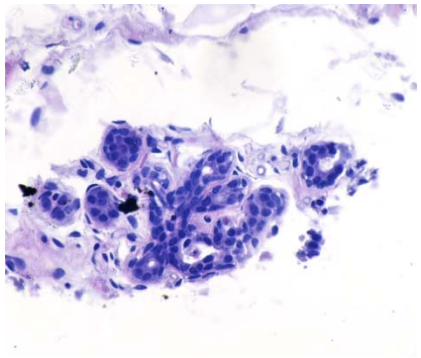

Template

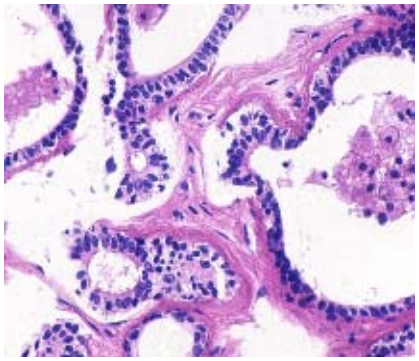

ColTrans

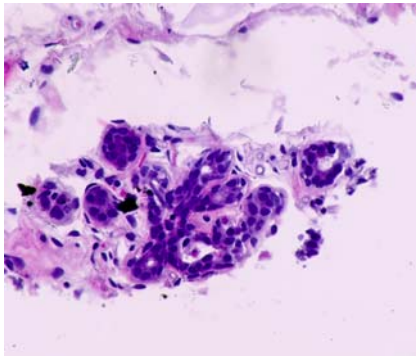

NMI: 0.6620, BiCC: 0.6134,
WsCC: 0.4109

PF

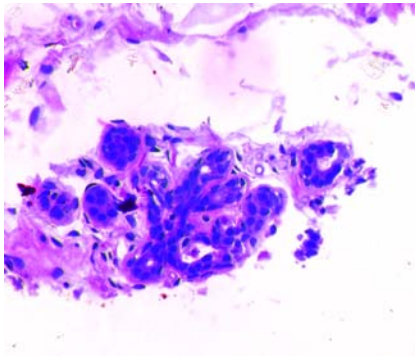

NMI: 0.6895, BiCC: 0.6578,
WsCC: 0.4552

EPF

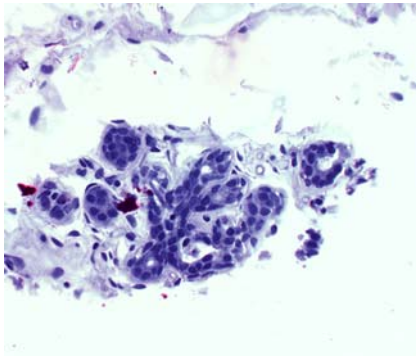

NMI: 0.6816, BiCC: 0.6484,
WsCC: 0.4438

Qualitative Analysis: Color Normalization

Source

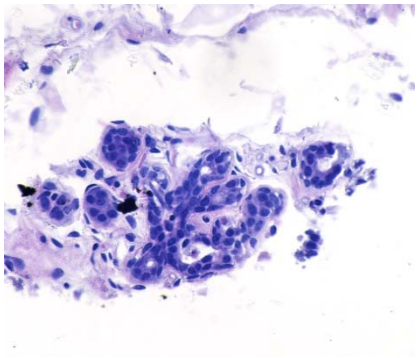

Template

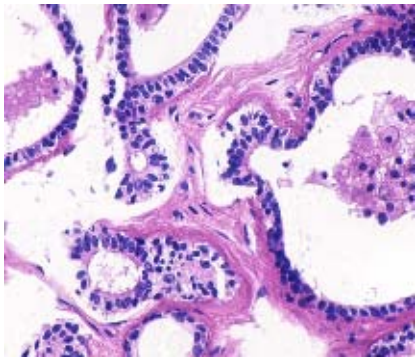

HTN

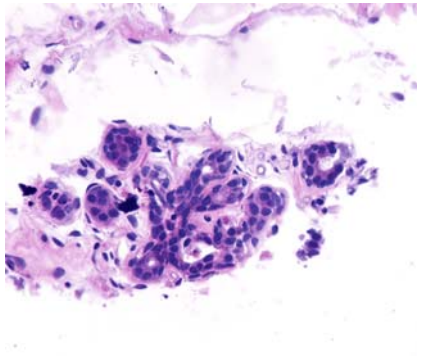

NMI: 0.7069, BiCC: 0.6745,
WsCC: 0.4776

SPCN

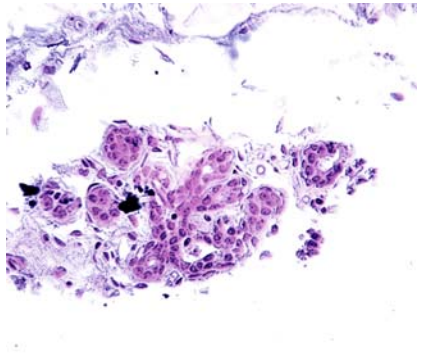

NMI: 0.6802, BiCC: 0.6476,
WsCC: 0.4416

SCD

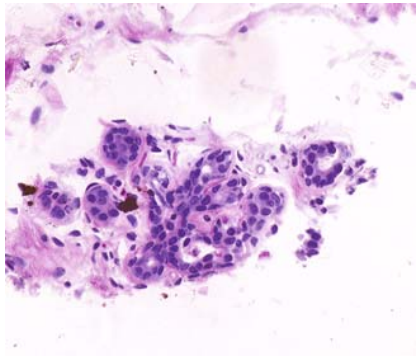

NMI: 0.6029, BiCC: 0.5664,
WsCC: 0.3471

Qualitative Analysis: Color Normalization

Source

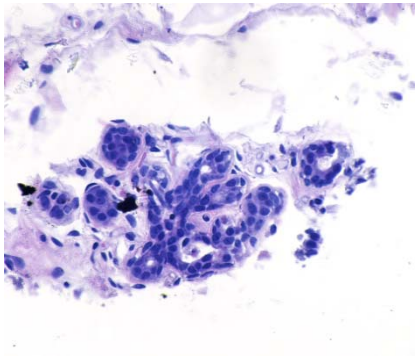

Template

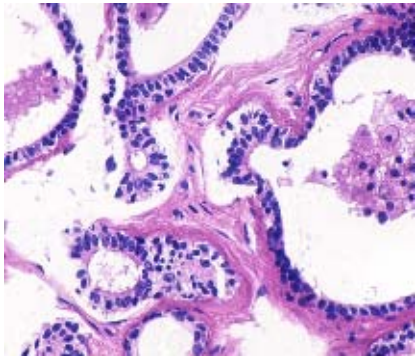

StainGAN

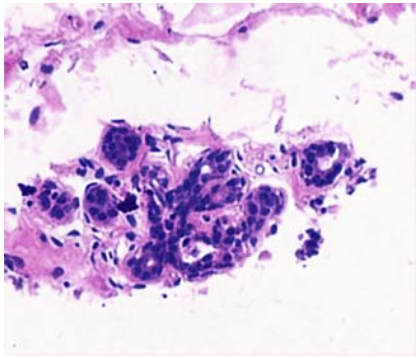

NMI: 0.6632, BiCC: 0.6255,
WsCC: 0.4174

AST

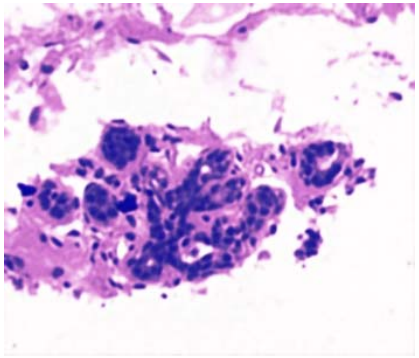

NMI: 0.6846, BiCC: 0.6439,
WsCC: 0.4418

SN-GAN

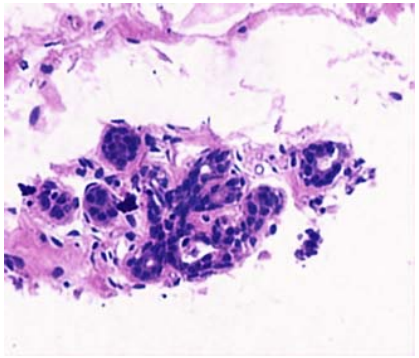

NMI: 0.7069, BiCC: 0.6702,
WsCC: 0.4743

Qualitative Analysis: Color Normalization

Source

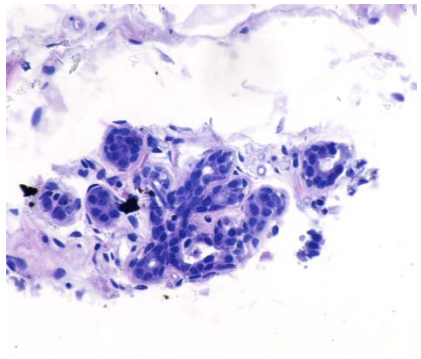

Template

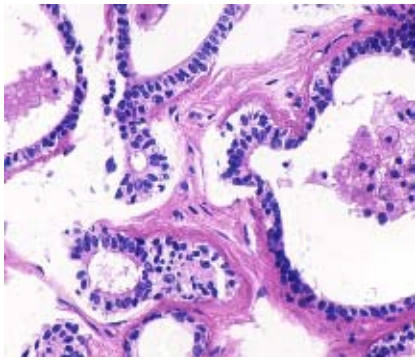

RFCC

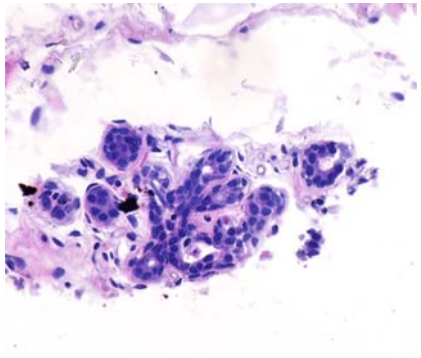

TredMiL

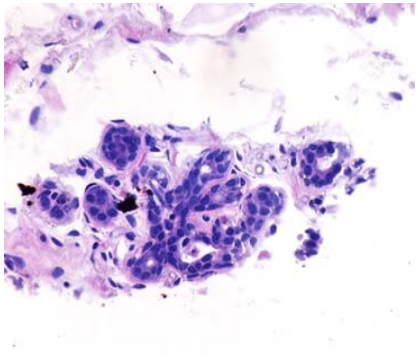

NMI: 0.7126, BiCC: 0.6925,
WsCC: 0.4925

NMI: 0.7547, BiCC: 0.7281,
WsCC: 0.5600

Performance Analysis

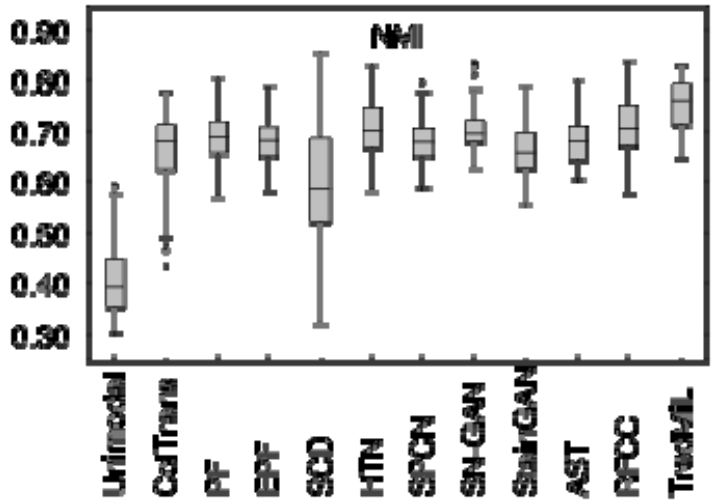

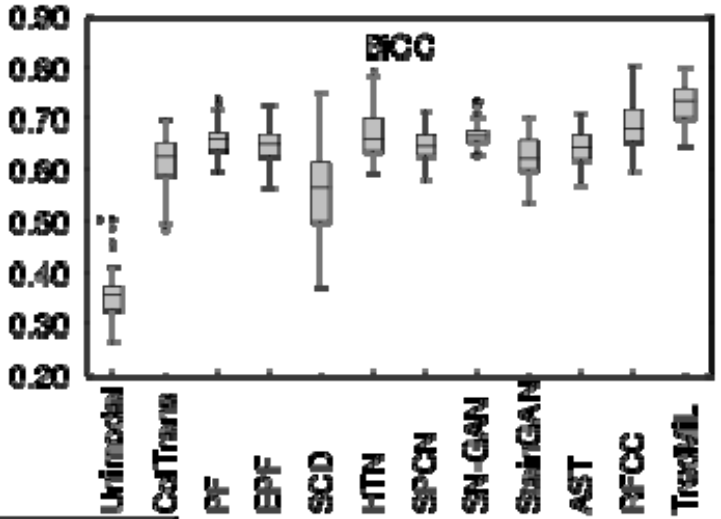

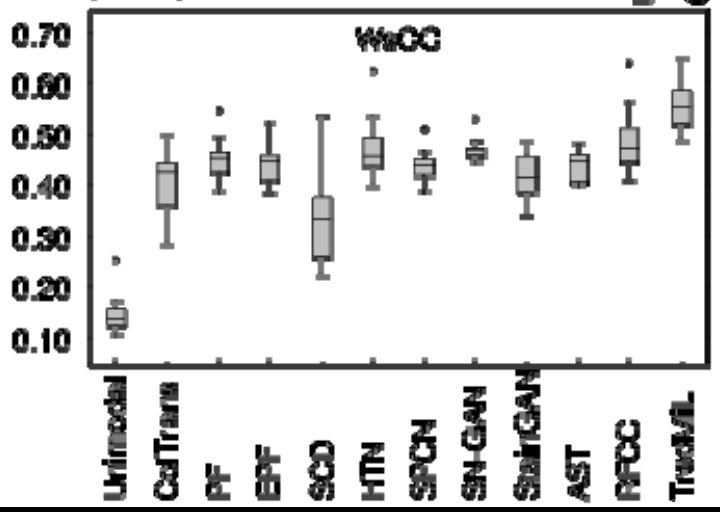

Color Normalization

Structural Similarity (SSIM Index)

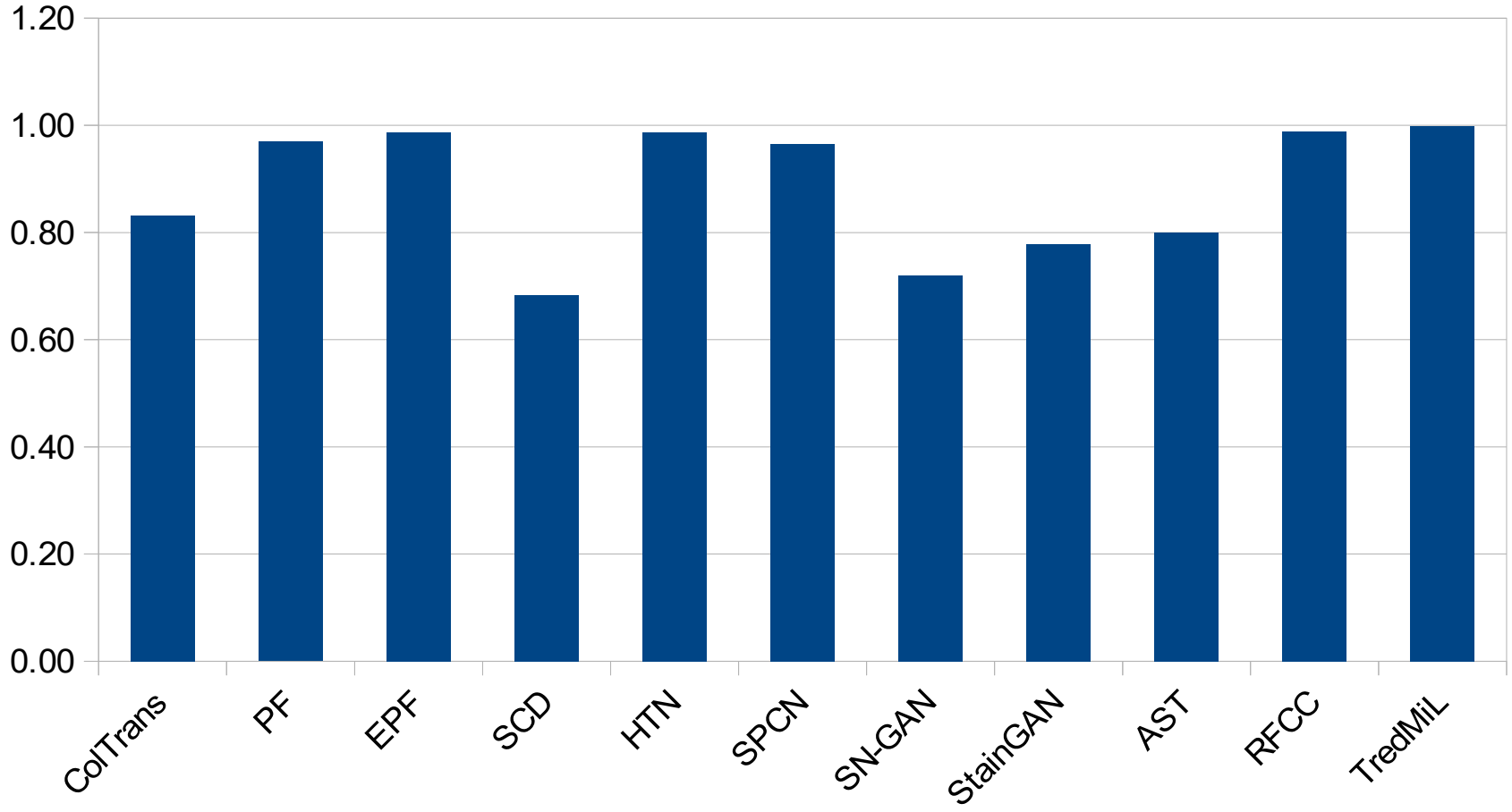

Z. Wang et al., "Image Quality Assessment: From Error Visibility to Structural Similarity", ***IEEE Transactions on Image Processing***, 13(4), pp. 600-612, 2004.

Limitations and Future Directions

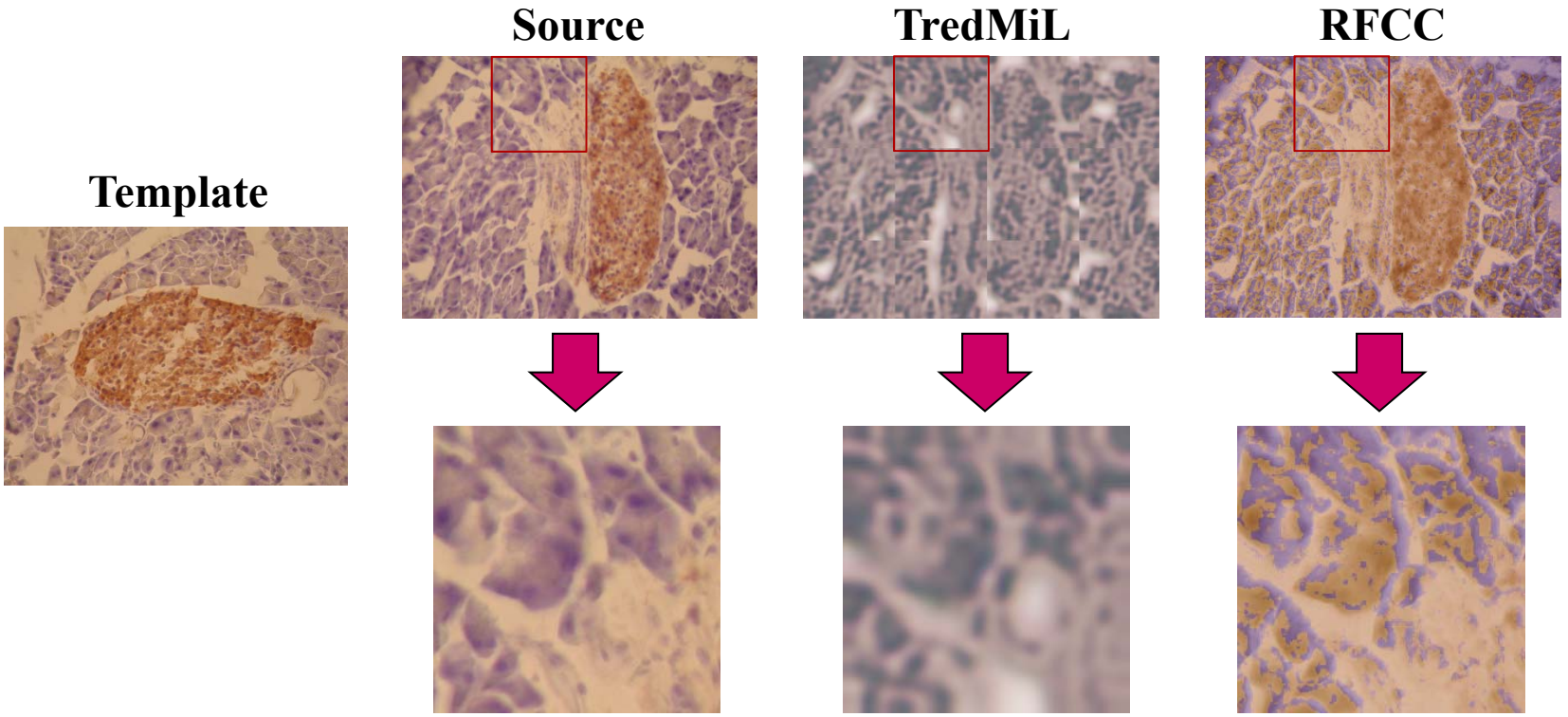

Haematoxylin-Diaminobenzidine (H&DAB) stained Warwick beta cell images

M. Kuse et al., "Local Isotropic Phase Symmetry Measure for Detection of Beta Cells and Lymphocytes", ***Journal of Pathology Informatics***, 2(2), pp. 2, 2012.

References

- M. T. Shaban *et al.*, "StainGAN: Stain style transfer for digital histological images", *Proceedings of International Symposium on Biomedical Imaging*, pp. 953-956, 2019.
- F. G. Zanjani *et al.*, "Stain Normalization of Histopathology Images using Generative Adversarial Networks", *Proceedings of International Symposium on Biomedical Imaging*, pp. 573-577, 2018.
- A. Bentaieb and G. Hamarneh, "Adversarial Stain Transfer for Histopathology Image Analysis", *IEEE Transactions on Medical Imaging*, 37(3), pp. 792-802, 2018.
- A. Vahadane et al., "Structure-Preserving Color Normalization and Sparse Stain Separation for Histological Images", *IEEE Trans. on Medical Imaging*, vol. 35, no. 8, pp. 1962-1971, 2016.
- X. Li and K. N. Plataniotis, "A Complete Color Normalization Approach to Histopathology Images Using Color Cues Computed From Saturation-Weighted Statistics", *IEEE Transactions on Biomedical Engineering*, vol. 62, no. 7, pp. 1862–1873, 2015.
- A. Khan, N. Rajpoot, D. Treanor, and D. Magee, "A Nonlinear Mapping Approach to Stain Normalization in Digital Histopathology Images Using Image-Specific Color Deconvolution", *IEEE Transactions on Biomedical Engineering*, vol. 61, no. 6, pp. 1729-1738, 2014.
- M. Macenko, M. Niethammer, J. Marron, D. Borland, J. T. Wooseley, X. Guan, C. Schmitt, and N. E. Thomas, "A method for normalizing histology slides for quantitative analysis", *IEEE International Symposium on Biomedical Imaging: From Nano to Macro*, pp. 1107-1110, 2009.
- E. Reinhard, M. Adhikhmin, B. Gooch, and P. Shirley, "Color transfer between images", *IEEE Computer Graphics and Applications*, vol. 21, no. 5, pp. 34-41, 2001.


Thank you